INVESTIGATION OF THE ACCURACY OF POST-PROCESSED STATIC GNSS DATA OF KNOWN POINTS USING CONSTELLATION DISCRIMINANT AT UNIVERSITY OF BENIN, UGBOWO CAMPUS, BENIN CITY

BY

MOSES, KELVIN AKHERE

ENV2002787

DEPARTMENT OF GEOMATICS

UNIVERSITY OF BENIN

BENIN CITY, NIGERIA

P.M.B 1154

SUBMITTED IN PARTIAL FULFILMENT OF THE REQUIREMENTS FOR THE AWARD OF A BACHELOR OF SCIENCES {BSCGEM - B.SC. GEOMATICS} DEGREE, IN THE FACULTY OF ENVIRONMENTAL SCIENCES, UNIVERSITY OF BENIN, BENIN CITY, EDO STATE, NIGERIA.

NOVEMBER 2025

INVESTIGATION OF THE ACCURACY OF POST-PROCESSED STATIC GNSS DATA OF KNOWN CONTROL POINTS USING CONSTELLATION DISCRIMINANT AT UNIVERSITY OF BENIN, UGBOWO CAMPUS, BENIN CITY

A PROJECT SUBMITTED BY

MOSES, KELVIN AKHERE

ENV2002787

SUBMITTED IN PARTIAL FULFILMENT OF THE REQUIREMENTS FOR THE AWARD OF A BACHELOR OF SCIENCES {BSCGEM - B.SC. GEOMATICS} DEGREE, IN THE FACULTY OF ENVIRONMENTAL SCIENCES, UNIVERSITY OF BENIN, BENIN CITY, EDO STATE, NIGERIA.

NOVEMBER 2025

CERTIFICATION

This is to certify that this project was carried out by **MOSES, KELVIN AKHERE** with Matriculation Number: **ENV2002787** of the Department of Geomatics, Faculty of Environmental Sciences, University of Benin, Edo State, Nigeria.

_____ _____

SUPERVISOR Date

Surv. Dr. P.E OJO

_____ _____

HEAD OF DEPARTMENT Date

Surv. Dr. S.O. Oladosu

---------- **----------**

EXTERNAL SUPERVISOR Date

DEDICATION

This project is dedicated to the Almighty God, the source of all creation, the architect of the universe, and the guide to all knowledge. Additionally, this research work is dedicated to my beloved father and mother, Mr. and Mrs. MOSES. Their unwavering support and encouragement profoundly influenced my academic journey.

ACKNOWLEDGEMENT

With a heart overflowing with gratitude, I thank Almighty God for the endless grace and mercy that nourished my journey. Deepest appreciation to my supervisor, Surv. Dr. P.E. Ojo, for your invaluable guidance. My profound thanks to the dedicated staff and management of the University of Benin's Department of Geomatics, particularly Prof. Raphael Irughe Ehigiator, Surv. Dr. Nwodo G.O, Surv. Dr S.O Oladosu, Surv. M.O Ekun, Surv. Dr. P.E Ojo, Dr. Alohan, Surv. Tijani, Surv. Dr. Joseph Odumosu, Engr. Mabel Alenkhe, Engr. Kelly Igbinidu, Mr Chuks as well as other staff of the department., for fostering a nurturing environment of knowledge and growth. To my dearest father, Pst. Moses Ikhuanegbe, and my unwavering Mom, Mrs. Bilikisu Moses, your boundless support has been the bedrock of my achievements. I extend my immense gratitude to Surv. Chika Vicent Okorocha, CEO of SACREDION NIGERIA LIMITED, for the invaluable mentorship and learning opportunities that fueled my development.

ABSTRACT

This study investigates the influence of satellite constellation configurations on the positional accuracy of post-processed static GNSS data at the University of Benin, Ugbowo Campus. Static observations were collected at five known control points using a Tersus David30 receiver. Data was processed in Tersus Geomatics Office across seven constellation setups: GPS-only, GLONASS-only, BEIDOU-only, and their combinations. A detailed epoch-based analysis was also conducted at one control point using RTKLIB. Accuracy was assessed using coordinate residuals (ΔE, ΔN, ΔH), RMSE, standard deviation, CEP, and 2DRMS, supplemented by classical and robust statistics and time-series analysis.

Results demonstrated that GPS-based solutions consistently delivered superior performance. The GPS+BEIDOU combination achieved the best accuracy (2DRMS = 0.160 m, CEP = 0.067 m), closely followed by GPS-only. In contrast, BEIDOU-only yielded the poorest results (2DRMS = 0.587 m), while GLONASS-only was notably weak and unstable. RTKLIB processing confirmed that multi-constellation setups, particularly GPS+GLONASS+BEIDOU, produced highly precise solutions with sub-centimeter standard deviations. Conversely, the GLONASS-only solution exhibited severe instability, with significant errors and outliers. Time-series analysis revealed that stable constellations maintained narrow error bands, while error spikes in other configurations corresponded directly to drops in satellite visibility.

Overall, the findings underscore the central role of GPS in precise positioning, highlight the stability benefits of integrated multi-constellation solutions, and expose the considerable limitations of standalone non-GPS constellations for high-accuracy applications.

Table of Contents

LIST OF TABLES

LIST OF FIGURES

CHAPTER ONE

INTRODUCTION

1.1 Background of the Study

The University of Benin (UNIBEN), established in 1970 in Benin City, Nigeria, is a major federal research university with two campuses: Ugbowo (main) and Ekehuan. The Ugbowo Campus alone houses over 44,000 students, multiple faculties, and the University of Benin Teaching Hospital (UBTH) (University of Benin, 2024). The campus blends open lawns, academic and administrative buildings, wooded areas, and infrastructure, forming a semi-structured environment that leads to intermittent GNSS signal obstruction and multipath effects that fall somewhere between ideal open-sky conditions and tightly built urban canyons (University of Benin, 2024; Akhigbe *et al.*, 2023).

Previous geodetic work at Ugbowo Campus has demonstrated reliable high-precision positioning. For instance, Ehigiator-Irughe and Oladosu (2023), densified first-order control points using CORS-referenced GNSS post-processing, achieving horizontal and vertical precisions on the order of millimeters. This confirms that millimeter-level accuracy is achievable in campus environments with appropriate surveying and analysis protocols.

While GNSS densification enhances positioning accuracy, understanding how different satellite constellation combinations influence static survey performance under the environmental and geometric conditions of Ugbowo Campus is essential for achieving optimal results. Integrating multiple constellations, such as GPS, GLONASS, Galileo, and BeiDou, provides increased satellite visibility, improved geometry (DOP), and greater redundancy, which are beneficial in partially obstructed environments (Sunusi *et al.*, 2024; Guo *et al.*, 2018). Research in similar semi-

urban contexts, like static PPP in Egypt and European settings, has shown that multi-constellation processing can yield centimeter-level improvements in positional accuracy compared to GPS-only setups (Guo *et al.*, 2018; Sunusi *et al.*, 2024).

Given the structural and vegetative complexity of the campus, understanding how constellation discrimination affects GNSS performance, especially in static post-processing, is vital. Constellation effectiveness may vary with session duration, obstructions, and receiver configuration, especially with modern multi-frequency, multi-constellation GNSS equipment. Evaluating GNSS data from Ugbowo Campus under different constellation configurations will provide empirical insights into optimal survey strategies in this context.

1.2 Statement of the Problem

While GNSS technology has become increasingly accessible and capable, the understanding of how to best configure multi-constellation receivers for specific survey environments is often limited among practitioners. In many field survey operations, receivers are either set to use default constellation combinations or configured based on anecdotal experience rather than empirical evaluation. This often results in inconsistent or suboptimal positioning outcomes, particularly in environments that experience moderate to high levels of signal obstruction or multipath, such as university campuses or urban landscapes.

At the Ugbowo Campus of the University of Benin, the built environment includes academic buildings, hostels, trees, and varying terrain, all of which can impact satellite visibility and signal quality. In such a scenario, the number of visible satellites and the strength of their signals can vary across different constellations. For example, GPS alone may not provide enough satellite geometry for a reliable solution at all times of the day, whereas combinations like GPS+GLONASS or GPS

+Galileo might improve availability and accuracy. However, without a scientific investigation, it is difficult to determine which constellation or combination yields the most reliable results under these conditions.

Furthermore, while CORS networks provide high-quality base station data for post-processing, the accuracy of the final static GNSS solution still largely depends on the quality and quantity of the satellite data collected during the field observation. As such, it is important to evaluate how each constellation or their combinations contribute to the overall accuracy of post-processed positions in the study area.

1.3 Aim and Objectives

This aim of this study is to investigate the accuracy of post-processed static GNSS data of known control points in University of Benin, Ugbowo campus by constellation discriminant approach.

The objectives are to:

I. process static GNSS data using different satellite constellation combinations, both individually and combined.

II. compare positional accuracy using coordinate differences (ΔE, ΔN, ΔH), Root Mean Square Error (RMSE), mean, standard deviation, 2D error, Circular Error Probable (CEP) and 2D RMS for each constellation across five control points from TGO result.

III. compute mean, RMSE, and both classical and robust statistical parameters to evaluate the positional accuracy of a 30-seconds RTKPOST epoch-based solutions.

IV. Analyze the time-series positional errors at a selected control point (GPS100) using fixed (Q=1) RTKPOST solutions.

1.4 Scope and Limitation of the Study

This study focuses on evaluating the positional accuracy of static GNSS observations using different satellite constellation combinations within the Ugbowo Campus of the University of Benin. Observations were carried out at multiple known control points using a Tersus David30 GNSS receiver mounted on a tribrach and tripod, with each point observed for one hour under static conditions.

The scope includes processing the collected data using Tersus Geomatics Office software, where each control point was analyzed using different constellation combinations such as GPS-only, GLONASS-only, BEIDOU-only, GPS+GLONASS, GPS+BEIDOU, GLONASS+BEIDOU, and all combined. Accuracy was assessed by comparing the processed coordinates to known reference values, using positional error metrics such as coordinate differences (ΔE, ΔN, ΔH), Root Mean Square Error (RMSE), 2D RMS, and Circular Error Probable (CEP).

In addition to the station-based analysis, a more detailed epoch-based assessment was performed on one control point (GPS100) using RTKLIB Demo 5L software. Here, the solution was processed at 30-second intervals for different constellations, focusing only on epochs with a fixed (Q=1) solution. This allowed for time series analysis and deeper insight into the variation of error over time.

While efforts were made to ensure accurate data collection, external factors such as multipath effects, signal obstructions from buildings or vegetation, and atmospheric conditions may have influenced the results. These factors were considered as general limitations but were not separately measured or analyzed in detail.

1.5 Justification of the Study

The precision and reliability of GNSS positioning are critical to the success of modern geospatial and engineering applications. As GNSS equipment continues to evolve, the integration of multiple satellite constellations has opened up new possibilities for improving positioning accuracy, satellite visibility, and survey reliability. However, while manufacturers promote multi-constellation capabilities, the actual performance of different constellation combinations remains highly dependent on environmental factors and location-specific conditions. There is, therefore, a pressing need for contextual studies that examine how these satellites systems behave under real-world conditions, particularly in environments that pose potential challenges to satellite visibility, such as university campuses.

Ugbowo Campus of the University of Benin presents a typical scenario where GNSS performance can be compromised by partial obstructions, such as buildings, tree cover, and localized terrain variations. Understanding how each GNSS constellation performs individually and in combination in this environment will contribute to academic research and also contribute practical insights that are directly applicable to surveying and geospatial workflows within similar urban or semi-urban areas.

Moreover, many geospatial practitioners still rely heavily on GPS-only configurations, often overlooking the potential improvements that can be gained by incorporating additional constellations such as GLONASS, Galileo, or BeiDou. By quantifying and comparing the accuracy of these configurations, this study will offer empirical evidence that can guide best practices in GNSS setup, equipment usage, and post-processing procedures.

This research also aligns with the broader goal of fostering data quality assurance in spatial data acquisition. As accurate georeferencing becomes increasingly important for infrastructure planning, land administration, environmental monitoring, and academic research, the results of this study will contribute to the development of more robust and adaptable GNSS methodologies. Additionally, the project promotes the practical application of post-processing tools and analysis techniques (such as Tersus Geomatics Office, Excel, and Python), thereby strengthening technical competency and fostering innovation in the use of geospatial technologies

CHAPTER TWO

LITERATURE REVIEW

2.1 GNSS Constellations and Integration

Abd Rabbou and El Rabbany (2016), explored how combining multiple GNSS constellations could improve the accuracy of Precise Point Positioning (PPP). They looked at signals from GPS, GLONASS, Galileo, and BeiDou, and assessed their effect both individually and in various combinations. A major focus of their work was comparing two PPP processing techniques: the standard undifferenced method and a more refined approach known as the between-satellite single-difference (BSSD) model.

From their experiments, which were based on three-hour static sessions across several GNSS stations, they observed that adding GLONASS, Galileo, or BeiDou to GPS generally improved accuracy. However, the Galileo constellation at the time did not contribute significantly due to its limited number of satellites. BeiDou, when added to GPS, brought noticeable improvements, especially in positioning accuracy after 15 minutes, but still underperformed when used alone.

The most impressive results came from combining all four constellations. This multi-constellation setup offered clear gains in positioning accuracy compared to using GPS alone. Moreover, when they applied the BSSD method, accuracy improved even further, and convergence time, the time it takes for the solution to stabilize, was shortened. In essence, their findings support the use of multiple GNSS systems together, particularly when processed with more advanced models like BSSD.

This work is relevant to the present study because it highlights not only the value of integrating different satellite systems like GPS, GLONASS, and BeiDou, but also how processing techniques can influence positioning performance.

Angrisano *et al.* (2020) examined how different combinations of GPS, GLONASS, and Galileo affect the accuracy of static Precise Point Positioning (PPP) when processed using the open-source RTKLib software. Their study relied on high-quality input data, including precise satellite orbits and clocks, ionosphere-free corrections, tidal corrections, and differential code biases from established international services. Two tropospheric modeling approaches were tested, the Saastamoinen model and an estimated Zenith Tropospheric Delay (ZTD) model to understand how atmospheric modeling influences results.

They processed two datasets: one from a permanent GNSS station operating continuously for a month, and another from a geodetic receiver collecting shorter daily sessions over ten days. By analyzing daily PPP solutions, they assessed accuracy, stability, and outlier handling.

Results showed that GPS-only and GLONASS-only performed at a similar level, while Galileo-only solutions lagged slightly behind. Combining constellations consistently improved accuracy, with GPS+Galileo emerging as the best dual-constellation choice. As expected, the triple combination of GPS, GLONASS, and Galileo delivered the highest precision, errors of only a few millimeters in the long-session dataset, and slightly larger errors for the shorter sessions. The estimated ZTD tropospheric model outperformed the Saastamoinen model, and using high-rate precise clock data at 30-second intervals instead of 15-minute intervals significantly boosted PPP accuracy, cutting GPS-only 3D error roughly in half.

This work reinforces the value of integrating multiple GNSS constellations, particularly in static surveys, and demonstrates how refined modeling choices and higher-rate precise products can yield substantial accuracy gains.

Kabir *et al.* (2016) compared the performance of single-GNSS and multi-GNSS receivers under various Korean agricultural environments, open fields, orchards, and mountainous areas, using both stationary and moving tests. The single-GNSS receiver (Hemisphere R100 DGPS) showed 2DRMS values of 0.162 m, 0.196 m, and 1.720 m in stationary mode across the three environments, while the multi-GNSS receiver (JAVAD SIGMA-G3T) in PPP mode with QZSS signals achieved superior accuracy, with 2DRMS values of 0.077 m, 0.162 m, and 0.929 m. In moving tests, RMSE values for the single-GNSS ranged from 0.168 m in open fields to 1.372 m in mountainous areas, whereas the multi-GNSS achieved RMSE values from 0.152 m to 1.13 m. The multi-GNSS consistently tracked more satellites than the single-GNSS in all scenarios, demonstrating its advantage in challenging environments. This study offers insights into selecting optimal GNSS configurations for agricultural applications.

Pan *et al.* (2017) investigated the performance of single-frequency Precise Point Positioning (PPP) using GPS, GLONASS, BeiDou, and Galileo, both individually and in combination. Using datasets from 47 globally distributed MGEX stations over seven days and additional kinematic data, they compared four-constellation single-frequency PPP (FCSF-PPP) with GPS-only and GPS/GLONASS PPP. The results showed that integrating multiple constellations significantly enhanced positioning accuracy compared to single-constellation solutions.

Prol *et al.* (2024) introduced HASlib, an open-source library for decoding Galileo High Accuracy Service (HAS) corrections, and demonstrated its integration with RTKLIB to enable decimeter-level real-time Precise Point Positioning (PPP) using standard GNSS receivers. Testing in Finland

showed a 3D RMS error below 20 cm (1σ) after 10–90 minutes of convergence, surpassing traditional real-time broadcast and SBAS-based solutions by an order of magnitude. While convergence took longer than post-processed multi-GNSS PPP due to RTKLIB filtering and high-latitude geometry limitations, once stabilized, sub-decimeter horizontal and vertical accuracy was achieved. This confirms Galileo HAS, when combined with open-source tools, as a cost-free, high-accuracy PPP solution.

Garcia *et al.* (2019) analyzed the performance of GNSS positioning using different satellite constellation combinations. Data were processed in RTKLIB through both single and relative positioning methods. Results showed that horizontal accuracy in single positioning improved when GPS was combined with BeiDou, whereas adding GLONASS and/or Galileo degraded positioning performance. In relative positioning, including Galileo, BeiDou, and QZSS also reduced accuracy. For vertical positioning, Galileo-only solutions showed the poorest performance, with height errors reaching approximately 4 m. Their study highlights that while multi-constellation integration can enhance positioning, certain combinations may worsen accuracy depending on processing conditions.

Ogutçu (2020) compared GPS+GLONASS static solutions with and without Galileo and found that including Galileo reduced horizontal RMS errors by roughly 11–16% (northing/easting) and also lowered maximum errors in a one-week SPP campaign. Xia *et al.* (2019) similarly reported that adding Galileo to GPS in static PPP improved the 2D position accuracy by about 25% in the east component (versus GPS alone). Pırtı *et al.* (2023) evaluated an all-constellation static solution (GPS + GLONAS S+ Galileo + BeiDou +QZSS) and concluded that full multi-GNSS processing achieved sub-decimeter accuracy (0–120 mm) after three days of observation, outperforming any single-constellation solution. In short, nearly all studies agree that every additional constellation

(GLONASS, Galileo, BeiDou, etc.) increases the satellite count and redundancy, which shortens solution convergence and reduces position errors relative to GPS-only processing.

In practical tests, these multi-constellation benefits are especially pronounced in short static occupations or poor-sky conditions. Steer (2021) demonstrated that for static surveys of only 1-6 hours duration, using all available GNSS constellations (GPS, GLONASS, Galileo, BeiDou, QZSS) dramatically lowered the number of failed ambiguity resolutions and cut 2D RMS errors compared to GPS-only sessions. Likewise, Pandey *et al.* (2016) showed that even with 5-10 min "rapid static" sessions, GPS+GLONASS processing still achieved centimeter-level accuracy where GPS-alone did not.

2.2 Static Positioning & Accuracy Evaluation

Correa Muñoz and Cerón Calderón (2018) assessed the precision and accuracy of static GNSS positioning for georeferencing surveying networks in civil engineering. Using dual-frequency equipment and applying differential corrections, they examined the effects of occupation time, time of day, and coordinate type. Under ideal conditions without multipath interference, the static method achieved a global RMSE of 1 cm, while points near buildings reached 4 cm. Optimal accuracy was obtained with 30-minute occupation times, and the authors emphasized the use of planar Cartesian coordinates for compatibility with distance-measuring surveys. Their findings support the suitability of static GNSS for establishing precise geodetic control networks.

Garcia *et al.* (2019) evaluated the positional accuracy of different single and multi-GNSS combinations using both single and relative positioning methods with survey-grade receivers. Post-processing in RTKLIB revealed that for single positioning, horizontal accuracy improved when GPS was combined with BeiDou, but degraded when GLONASS and/or Galileo were added.

In relative positioning, the inclusion of Galileo, BeiDou, and QZSS generally reduced accuracy. Notably, Galileo-only single positioning produced significant vertical errors, with a displacement of about 4 meters from the mean height. The study highlights that optimal GNSS constellation selection depends on the positioning method and the desired accuracy.

Purfürst (2022) investigated the static autonomous GNSS positioning accuracy of smartphones under forest canopy conditions, comparing four multi-frequency, multi-constellation models, six single-frequency smartphones, and a geodetic receiver. Data collection took place at 15 forest sites, with 24 measurements of roughly 10 minutes each for all devices. Results showed that, on average, multi-frequency smartphones provided better accuracy than single-frequency models. However, performance varied significantly among devices, even between identical models, indicating that accuracy cannot be generalized based solely on frequency or constellation support. The dual-frequency Xiaomi Mi 10 was the top performer, achieving a DRMS of 4.56 m and a 34% lower absolute error than the best single-frequency phone.

2.3 GNSS PPP/PPP-RTK and Post-Processing Methods

Dawidowicz and Bakuła (2023) evaluated the potential of open-source software for achieving high-accuracy Precise Point Positioning (PPP), focusing on the impact of BeiDou observations within Europe. Using ten days of multi-GNSS data processed in GAMP, they analyzed position accuracy across varying observation session lengths and satellite system combinations. Despite BeiDou's incomplete visibility in Europe, adding its observations, particularly when combined with GLONASS or Galileo, significantly improved positioning accuracy, especially for short sessions between 30 minutes and two hours. Improvements were evident in both reduced coordinate deviations and lower standard deviations. The findings confirm GAMP's effectiveness

for multi-GNSS PPP analysis and highlight BeiDou's contribution even in regions with limited satellite coverage.

Hou and Zhou (2023) conducted a global-scale evaluation of positioning accuracy (RMS) and convergence time for GPS, BDS-3, and Galileo using Precise Point Positioning (PPP). GPS demonstrated the best overall performance worldwide, while Galileo and BDS-3 showed competitive results only in specific latitude regions. Combining two constellations generally improved performance over single-system solutions, with the Galileo–BDS-3 pairing achieving up to a 50% improvement in RMS and convergence time compared to either alone, especially in kinematic PPP. For GPS, dual-system combinations with Galileo or BDS-3 brought minimal gains. The study also examined how different precise products from MGEX analysis centers influenced PPP results, finding that GRG products delivered the best accuracy for GPS, while COD products were optimal for Galileo and BDS-3. Depending on the product choice, performance differences could reach 2 cm in RMS and 15 minutes in convergence time.

Li *et al.* (2019) explored the potential of triple-frequency PPP ambiguity resolution (AR) using BDS and Galileo constellations. Their study evaluated B1, B2, and B3 signals from BDS, alongside E1, E5a, and E5b signals from Galileo, to assess improvements in positioning accuracy. The authors estimated uncalibrated phase delay (UPD) products and analyzed their stability across 30 days. Results showed that extra-wide-lane (EWL) and wide-lane (WL) UPDs were stable for both systems, while narrow-lane (NL) UPDs exhibited minimal fluctuations. Galileo UPDs demonstrated higher reliability compared to BDS, attributed to better observation quality. Importantly, the study found that incorporating triple-frequency PPP AR improved positioning accuracy by 30-70% over ambiguity-float solutions, in both static and kinematic modes. Furthermore, triple-frequency fixed solutions outperformed dual-frequency fixed solutions in both

convergence time and accuracy, particularly for Galileo-only and combined BDS–Galileo configurations. Overall, the fusion of multi-GNSS signals enhanced position estimation by leveraging improved satellite geometry and availability.

Researchers have recently evaluated the feasibility of combining low-cost GNSS receivers with the Galileo High Accuracy Service (HAS) for real-time Precise Point Positioning (PPP). Galileo HAS is a free augmentation service provided by the European Union, targeting accuracies of 20 cm horizontally and 40 cm vertically (95% confidence level) within 300 seconds. While such performance had already been confirmed with geodetic-grade receivers, mass-market applications require testing with low-cost receivers and antennas. Marut *et al.* (2024) investigated this by assessing real-time static and kinematic positioning with GPS + Galileo dual-frequency setups. Their findings showed that Galileo HAS SL1 corrections enabled both geodetic-grade and low-cost receivers to achieve the target accuracy in open-sky conditions. Specifically, static positioning reached centimeter-level precision, while kinematic positioning maintained sub-decimeter accuracy. The main limitation observed was in vertical accuracy due to the lack of antenna phase center offset models for low-cost hardware. Overall, the study demonstrates that pairing low-cost receivers with Galileo HAS can deliver results comparable to geodetic-grade systems, making it a viable solution for affordable, high-precision GNSS applications.

Zhang and Li (2024) conducted a comprehensive assessment of Galileo Single Point Positioning (SPP) using different broadcast ephemeris data sources. Their analysis revealed that the International GNSS Service (IGS) provides the highest completeness of navigation message records (ECR > 70%), while the Institut Géographique National (IGN) had the lowest. They further evaluated the proportions of different Galileo navigation message types within IGS broadcast ephemeris files, finding that FNAV_258 and INAV_517 exhibited better completeness, whereas

INAV_513 and INAV_516 were comparatively poorer. The study also compared SPP solutions between Galileo and GPS, showing that higher ECR values generally led to improved positioning accuracy. While GPS produced smoother results with smaller fluctuations, Galileo achieved higher SPP accuracy, particularly when dual-frequency observations were employed, which significantly reduced data dispersion and improved vertical accuracy.

Malik (2020) investigated how combining multiple GNSS constellations influences the performance of static Precise Point Positioning (PPP). Using seven days of data from seven MGEX stations, the study compared GPS-only, GLONASS-only, and various multi-constellation solutions, including GPS/GLONASS, GPS/GLONASS/Galileo, GPS/GLONASS/BeiDou, and GPS/GLONASS/Galileo/BeiDou. The findings revealed that integrating GLONASS with GPS improved positioning accuracy compared to GPS-only PPP, with standard deviations of 4.10 cm (east), 3.42 cm (north), and 6.50 cm (up). The combined GPS/GLONASS solution achieved a 3D RMS error of 8.96 cm. Further improvements were noted when Galileo and BeiDou were added, with the GPS/GLONASS/Galileo/BeiDou combination reaching a horizontal RMS of 5.35 cm. Interestingly, the inclusion of BeiDou provided only marginal improvements compared to Galileo. Convergence time also improved slightly (3.81%) when using GPS/GLONASS/Galileo, highlighting the value of multi-constellation PPP for higher accuracy and faster stabilization.

2.4 Static GNSS Positioning and Post-Processing

Static GNSS (Global Navigation Satellite System) surveys occupy a point for an extended time to achieve the highest accuracy in position. In static mode, a dual-frequency receiver collects carrier-phase and pseudo-range data while remaining stationary, and the resulting measurements are later processed relative to a known base station. Short baseline (local) static surveys, with base-rover separations of only a few meters to a few kilometers, yield very high precision because many errors

(satellite orbit/clock errors, atmospheric delays, multipath, etc.) are nearly common to both receivers and thus cancel in a differential solution. For example, Okorocha and Olajugba (2014), found that baselines ≤1.5 km gave the highest horizontal and vertical precision, whereas much longer baselines (~100 km) significantly degraded accuracyfig.net. In practice, static surveys typically use a single receiver (with a precise antenna) per point; the reference (base) may be an existing control station or a CORS (Continuously Operating Reference Station). The baseline vector between base (coordinates (X_b, Y_b, Z_b) and rover (Xr,Yr,Zr) is estimated by solving the GNSS observation equations, yielding $(\Delta X, \Delta Y, \Delta Z) = (Xr - Xb, Yr - Yb, Zr - Zb)$. Static networks underpin control surveying: the resulting coordinates define a local frame or tie to national datums when scaled across multiple baselines and control points.

Observations must be long and stable. Static surveys demand strict occupation protocols: the antenna must be firmly mounted on a survey tripod or fixed monument, and logging should be continuous. Observation durations vary by application: rapid-static surveys might occupy a point for 15 min-2 h, whereas full static (or CORS) occupations run several hours (or continuously). Longer sessions improve ambiguity resolution and precision. For example, Nwabueze (2020) recommends up to 2 h static sessions to obtain optimal height accuracy on first-order controls.

The post-processing step solves the GNSS observation equations differentially. A typical carrier-phase observation model for satellite *i* and a receiver A can be written as (Ezeigbo, 2022):

$$\Delta\varphi_{iA} = \frac{\rho_{iA}(t)}{\lambda} + \frac{c}{\lambda}\left(\delta_A(t) - \delta_i(t)\right) + I_{iA} + T_{iA} - N_{iA} + \epsilon_{\varphi} \qquad (2.1)$$

Where,

$\Delta\varphi_{iA}$ *is the* measured carrier phase (in cycles) between satellite *i* and receiver *A*

$\rho_{iA}(t)$ is the geometric range between receiver *A* and satellite *i* (in meters)

λ is the Carrier wavelength (in meters/cycle)

C is Speed of light in vacuum (~299,792,458 m/s)

$\delta_A(t)$ is the receiver clock bias (in seconds)

$\delta_i(t)$ *is the* satellite clock bias (in seconds)

I_{iA} is the ionospheric delay

T_{iA} *is the tropospheric delay*

N_{iA} *is the i*nteger ambiguity (number of full carrier cycles, unknown)

ϵ_φ *is the* measurement noise and multipath error on the phase observation

However, in simpler or idealized form (ignoring atmospheric errors):

$$\Delta\varphi_{iA} = \frac{\rho_{iA}(t)}{\lambda} + \frac{c}{\lambda}\left(\delta_A(t) - \delta_i(t)\right) - N_{iA} \quad (2.2)$$

In a double difference model between two receivers A and B and two satellites i and j, the observation model takes the form of equation (1.3):

$$\nabla\Delta\varphi_{iAB}(t) = \frac{1}{\lambda}\Delta\rho_{iAB}(t) + \frac{c}{\lambda}\nabla\delta_{AB}(t) - \nabla N_{iAB} \quad (2.3)$$

$$\nabla\Delta\varphi_{jAB}(t) = \frac{1}{\lambda}\Delta\rho_{jAB}(t) + \frac{c}{\lambda}\nabla\delta_{AB}(t) - \nabla N_{jAB} \quad (2.4)$$

From equation (1.2) and (1.3), the double difference ($\nabla^2\Delta\varphi_{ijAB}$) *is given by*:

$$\nabla^2\Delta\varphi_{ijAB}(t) = \nabla\Delta\varphi_{iAB}(t) - \nabla\Delta\varphi_{jAB}(t) \quad (2.5)$$

$$\nabla^2\Delta\varphi_{ijAB}(t) = \frac{1}{\lambda}(\Delta\rho_{iAB}(t) - \Delta\rho_{iAB}(t)) - (\nabla N_{iAB} - \nabla N_{jAB}) \quad (2.6)$$

Hence,

$$\nabla^2\Delta\varphi_{ijAB}(t) = \frac{1}{\lambda}\nabla^2\rho_{ijAB}(t) - \nabla^2 N_{ijAB} \quad (2.7)$$

In this model, the receiver and satellite clock errors are eliminated.

In the triple difference model between two receivers A and B and two satellites i and j, at two epochs t_1 and t_2, the observation model takes the form of equation (1.7):

$$\nabla^2\Delta\varphi_{ijAB}(t_1) = \frac{1}{\lambda}\nabla^2\rho_{ijAB}(t_1) - \nabla^2 N_{ijAB} \quad (2.8)$$

$$\nabla^2\Delta\varphi_{ijAB}(t_2) = \frac{1}{\lambda}\nabla^2\rho_{ijAB}(t_2) - \nabla^2 N_{ijAB} \quad (2.9)$$

Subtracting the equations (1.7) and (1.8), we have

$$\nabla^3\Delta\varphi_{ijAB}(t_{12}) = \nabla^2\Delta\varphi_{ijAB}(t_1) - \nabla^2\Delta\varphi_{ijAB}(t_2) \quad (2.10)$$

$$\nabla^3\Delta\varphi_{ijAB}(t_{12}) = \frac{1}{\lambda}\nabla^2\rho_{ijAB}(t_1) - \nabla^2 N_{ijAB} - (\frac{1}{\lambda}\nabla^2\rho_{ijAB}(t_2) - \nabla^2 N_{ijAB}) \quad (2.11)$$

$$\nabla^3\Delta\varphi_{ijAB}(t_{12}) = \frac{1}{\lambda}(\nabla^2\rho_{ijAB}(t_1) - \nabla^2\rho_{ijAB}(t_2)) \quad (2.12)$$

$$\nabla^3\Delta\varphi_{ijAB}(t_{12}) = \frac{1}{\lambda}(\nabla^3\rho_{ijAB}(t_{12})) \quad (2.13)$$

Where the parameters have been defined in equation 2.1

This model is also referred to as the ambiguity free model. That is, equation (2.13) is free of ambiguity parameters. Hence, in addition to being free from satellite and clock errors, it is also independent of the integer ambiguity.

2.5 Research Gaps and Relevance to Current Study

Over the years, static GNSS positioning has been rigorously examined in a variety of environmental and operational contexts. However, much of the existing research has focused on open-sky or heavily urbanized settings, where signal behavior and satellite geometry differ significantly from mixed environments like university campuses. These studies have often concentrated on improving ambiguity resolution, assessing the accuracy of PPP and RTK solutions, or analyzing the benefits of multi-constellation and multi-frequency integration using high-end receivers under ideal or highly obstructed conditions.

In environments such as Ugbowo Campus, characterized by partial obstructions, open green spaces, trees, and buildings, GNSS signals behave in more complex ways, influenced by intermittent multipath, variable satellite visibility, and localized atmospheric conditions. Although such environments are not fully urban, they still present non-trivial signal challenges that affect the reliability and repeatability of static positioning, particularly for high-precision geospatial tasks. Evaluating static post-processed GNSS accuracy under these real-world, semi-obstructed conditions offers practical insights that extend beyond what is typically observed in controlled or extreme environments.

Furthermore, while multi-constellation GNSS has become standard in most modern receivers, the extent to which combining constellations (e.g., GPS, GLONASS, Galileo, BeiDou) enhances positioning performance can vary across local settings. Factors such as satellite geometry, DOP variation throughout the day, and the influence of antenna setup or observation time play a substantial role in the quality of derived positions. This study considers these elements within the specific context of Ugbowo Campus, aiming to assess how post-processing techniques and observation strategies affect positional accuracy in practice.

In addition, although several studies have reported the effectiveness of using longer observation durations and advanced processing software in achieving centimeter-level accuracy, fewer have evaluated the comparative performance of such methods in semi-structured environments like university campuses in West Africa. This research takes into account the tools and receivers accessible in such regions and examines how they perform under realistic field constraints.

By investigating post-processed static positioning with attention to constellation selection, session duration, environmental context, and data processing methodology, the current study contributes context-specific understanding to an already well-developed area of GNSS research.

CHAPTER THREE

METHODOLOGY

3.1 Description of the Study Area

This study was carried out within the Ugbowo Campus of the University of Benin (UNIBEN), located in Benin City, the capital of Edo State, in Nigeria's South-South geopolitical zone. The campus is geographically positioned between latitude 6°23′30″ N and 6°24′30″ N, and longitude 5°36′30″ E and 5°38′00″ E, with a central coordinate approximately at 6°23′50″ N, 5°37′23″ E. Ugbowo Campus straddles Egor Local Government Area and Ovia North-East Local Government Area, and it lies adjacent to the Benin-Lagos Expressway.

Originally established in 1970 as the Institute of Technology, the University was granted full university status by the National Universities Commission (NUC) in 1971 and renamed the University of Benin in 1972. It later became a federal university. The campus hosts over 45,000 students, comprising both full-time and part-time enrolments across diverse academic disciplines. The institution is home to faculties such as Engineering, Life Sciences, Environmental Sciences, Agriculture, Education, Law, Physical Sciences, Pharmacy, Arts, and Social Sciences, all situated within the main campus at Ugbowo.

Topographically, the campus is generally flat, with slight elevation variation ranging between 45 and 60 meters above mean sea level, based on recent GNSS observations. The area is bounded to the north by the Ekosodin community, to the west by the Edo Development and Property Agency (EDPA) Estate, and to the east, across the Ikpoba River, by Akiuwa and Edosowan communities. The southern boundary includes a mix of academic and residential developments.

The physical environment of the campus is characterized by a mixture of open spaces, vegetated corridors, and clusters of one to multi-storey buildings, including lecture halls, laboratories, hostels, and administrative blocks. Internal roads, shaded walkways, and landscaped lawns further define the spatial layout.

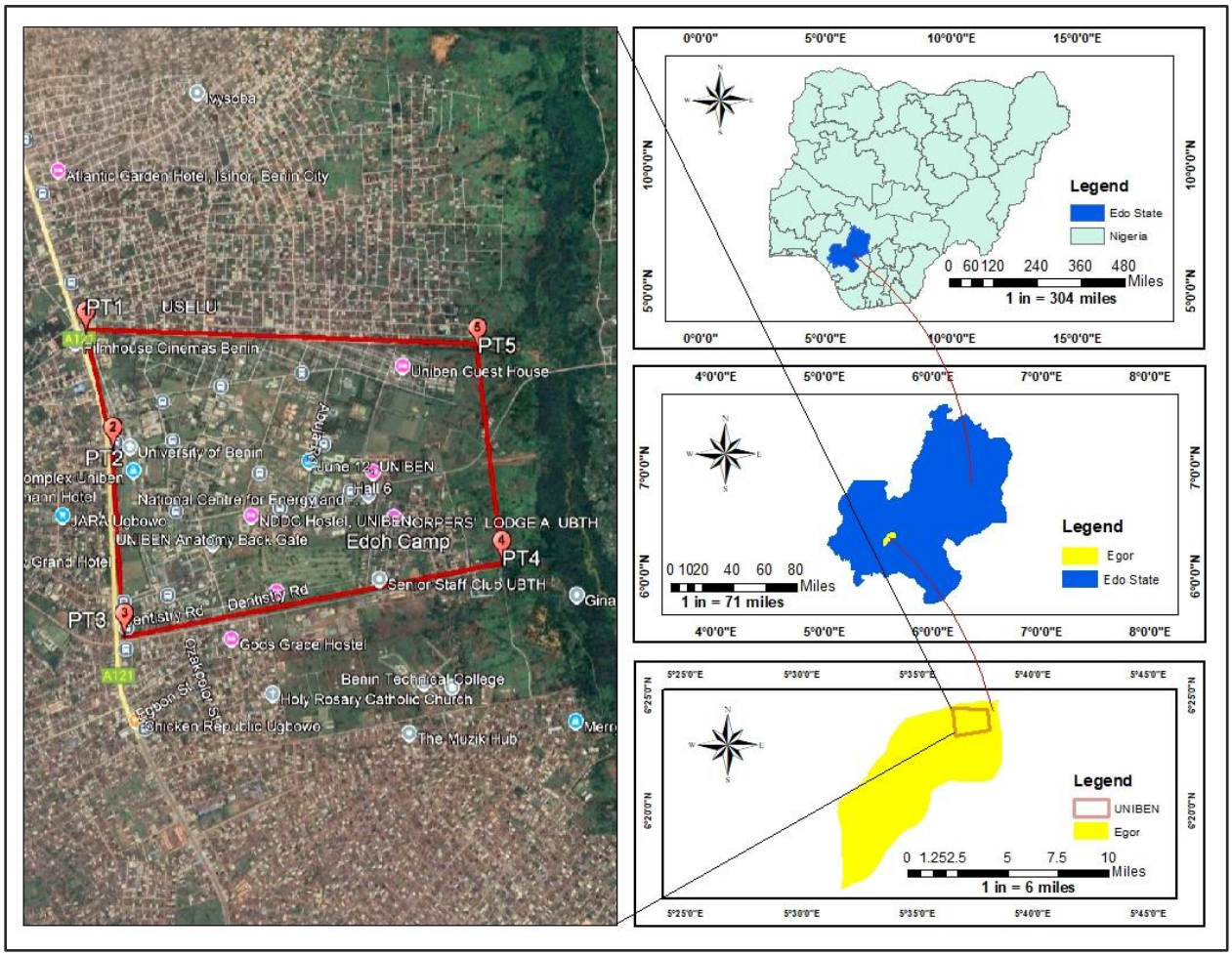

Figure 3.1 Study Area Map of University of Benin and It's Environment

3.2 Data Sources

The data for this study was collected using Tersus David 30 GNSS receivers under static survey conditions at the University of Benin's Ugbowo Campus. To account for diverse environmental factors, observations were made on five control stations strategically located across the campus.

These locations represented varied conditions, including areas with partial obstructions, open skies, and dense vegetation.

At each of the control points (RaphUNB01, RaphUNB02, UNIBEN01, UNIBEN02, and GPS100), static GNSS observations were continuously recorded for one hour at a 5-seconds epoch interval. The raw GNSS data, which included both pseudo-range and carrier-phase measurements, was logged in its native format. Subsequently, the Tersus RINEX converter was used to convert this raw data into RINEX files for each station, precisely aligning with their respective start and end observation times.

To enhance positional accuracy and ensure solution integrity, correction data from GeoSys Continuously Operating Reference Station (CORS) was incorporated. This CORS station supplied precise positional corrections, orbital information, and timing data, which are crucial for high-accuracy post-processing. This differential correction significantly improved the reliability of the coordinate computations.

Post-processing was performed using Tersus Geomatics Office software and RTKLIB Demo 5L. This software allowed for the import of the RINEX files, the application of the CORS-based corrections, and the filtering of satellite constellations to facilitate comparative analysis. The software supported various constellation-specific solutions, including GPS-only, GLONASS-only, BEIDOU-only, GPS + GLONASS, GPS + BEIDOU, GLONASS+BEIDOU and combined multi-GNSS configurations.

The primary datasets utilized in this study include:

I. Raw GNSS observation files (RINEX) obtained from the static survey sessions.

II. Correction data from GeoSys CORS station, providing high-quality differential input for enhanced post-processed positioning.

III. Reference coordinates of the control points, serving as benchmarks for evaluating accuracy.

IV. Processing outputs from Tersus Geomatics Office and RTKLIB Demo 5L.

The coordinates of the control points in UTM Zone 31 (WGS84) are given by the table below:

Table 3.1 UTM Coordinate of Control Points

Stations	Eastings (m)	Northings (m)	Height (m)
RAPHUNB01	789774.1402	708303.8314	121.1585
RAPHUNB02	789804.4312	708399.3471	120.6859
UNIBEN01	789633.0081	708612.0767	124.0336
UNIBEN02	789875.7324	708645.7109	119.1559
GPS100	789397.9902	708576.4309	127.3695

3.3 GNSS Survey Planning

GNSS survey planning is an essential step in this research to ensure that satellite observations are collected during periods of optimal satellite visibility and favorable geometric conditions. This planning is particularly important given the study's focus on satellite constellation discrimination and positional accuracy.

Prior to field data collection, the Trimble GNSS Online Planning Tool was used to predict satellite availability and estimate DOP (Dilution of Precision) values for the Ugbowo Campus (approx. 6°23′50″ N, 5°37′23″ E). The tool allows for the simulation of satellite positions for multiple constellations, including GPS, GLONASS, Galileo QZSS, and BeiDou, over a specified time window. An elevation mask of 15° is applied to exclude satellites too close to the horizon, which are typically more prone to atmospheric interference and multipath effects.

The planning process involves selecting a 24-hour period and analyzing:

I. Predicted PDOP, HDOP, and VDOP values

II. Predicted Sky Plot for all satellite constellations

III. Number of visible satellites per constellation

Based on this analysis, observation sessions were scheduled during periods of high satellite availability (typically ≥ 12 satellites) and low PDOP values (ideally ≤ 2.0), which are conducive to achieving high-accuracy static positioning results.

Sky plots and DOP graphs generated from the tool were saved and referenced in this study to justify the timing of each observation session.

By integrating Trimble GNSS planning online tool into the survey methodology, this study ensures consistency, avoids poor satellite configurations, and enhances the integrity of the collected GNSS data.

A uniform cut-off angle, with a default value of 15° was chosen, to avoid signals with atmospheric distortion and possible multipath errors at low elevations (Leick et al., 2015).

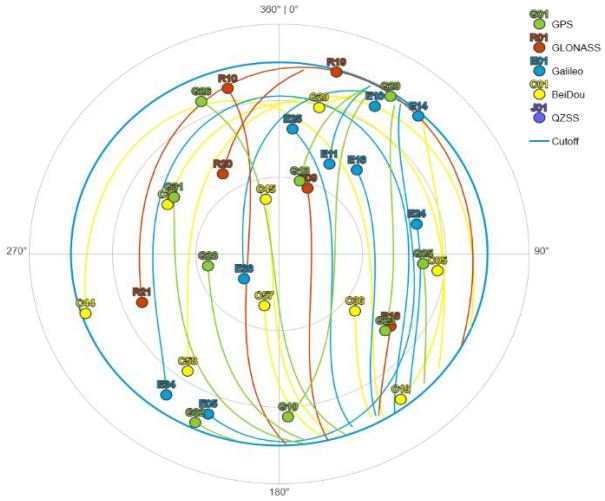

Figure3.2: Predicted Skyplot for Multi-GNSS Visibility over Ugbowo Campus (Elevation Mask: 15°)

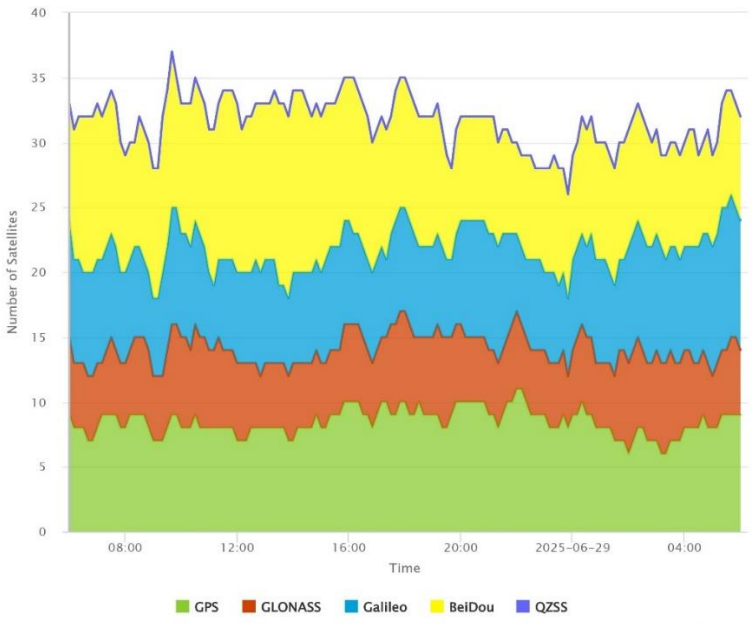

Figure 3.3: Predicted Satellites Counts from Trimble GNSS Online Planning Tool

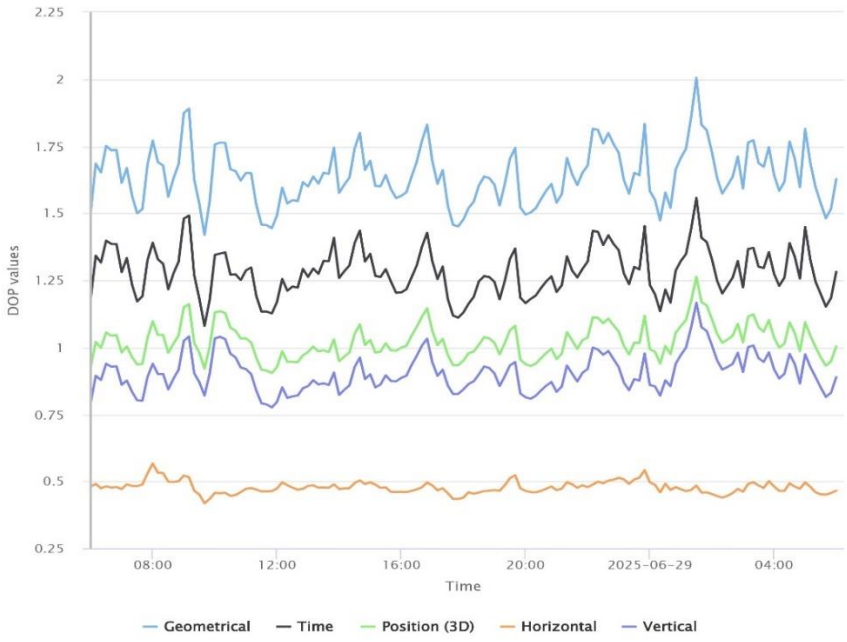

Figure 3.4: DOPs Variation over 24 Hours from Trimble GNSS Online Planning Tool

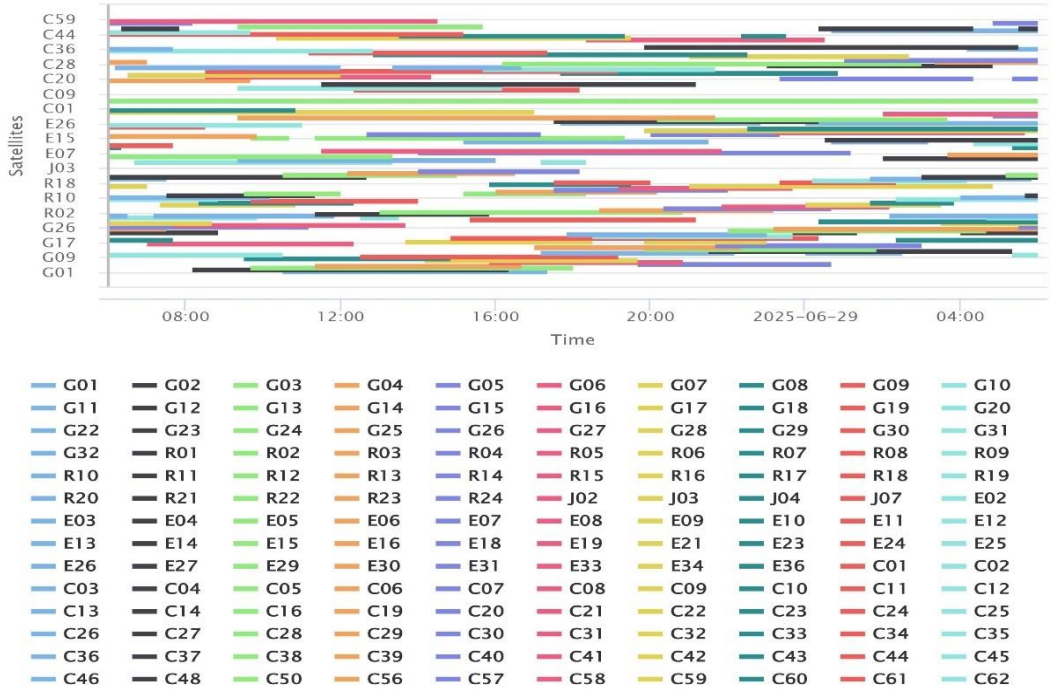

Figure 3.5: Predicted Satellites Visibility from Trimble GNSS Online Planning Tool

3.4 Data Collection

Data collection for this study was conducted using static GNSS survey techniques at five control stations within the Ugbowo Campus of the University of Benin. The campus provides a semi-urban environment with varied signal conditions, making it suitable for evaluating GNSS positioning performance under different satellite constellation configurations.

At each control station, a Tersus David30 GNSS receiver was mounted on a tribrach, which was then securely placed on a tripod to ensure vertical stability and centering over the survey point. This setup provides a solid foundation for long-duration static observations. The GNSS receiver operates in muti-frequency mode, recording both pseudo-range and carrier-phase raw observation data.

The antenna height was measured precisely from the control point to the Antenna Reference Point (ARP) on the Tersus David30 receiver setup. Since the receiver was mounted on a tribrach and tripod, the height was recorded using a tape measure to the nearest meters.

Observations were conducted for a continuous duration of one hour at each point, with an epoch interval of 5 seconds to capture high-resolution satellite data. The selected observation period was intended to ensure adequate satellite pass coverage, reduced temporal noise, and the ability to extract meaningful accuracy statistics across different constellation combinations.

Correction data was obtained from GeoSys Continuously Operating Reference Station (CORS) to support differential post-processing. This correction stream compensates for satellite orbit and clock errors and enhances the overall positional integrity of the static solution.

During each session, field notes were taken to document, weather conditions such as temperature and humidity, start and end time of observation and environmental conditions such as sky visibility,

surrounding obstructions, and multipath sources. Where necessary, photographs and field sketches were collected to provide contextual understanding of signal environments. The combination of raw GNSS data, and CORS corrections forms the input for post-processing and subsequent analysis of coordinate accuracy.

This approach ensures consistency across all control stations and enables rigorous analysis of how different satellite constellations (GPS, GLONASS, Galileo, BeiDou) influence the quality and precision of static GNSS positioning.

Table 3.2 Observation Details of Control Stations from Site

Station	Date	Time (UTC+1)	Antenna Height (m)	Temperature (°C)	Humidity (%)
RaphUNB01	28/06/2025	8:15AM – 9:15AM	1.15	25	96
RaphUNB02	28/06/2025	9:40AM – 10:40AM	0.954	26	92
UNIBEN01	28/06/2025	11:01AM – 12:01PM	1.059	28	85
UNIBEN02	28/06/2025	12:20PM – 13:20PM	0.796	27	86
GPS100	28/06/2025	13:32PM – 14:32PM	1.311	28	80

3.5 Post-Processing Procedures

Post-processing is a critical phase in this study, where raw GNSS data is refined to produce accurate positional results. During fieldwork, static observations were carried out at each control point using the Tersus David30 GNSS receiver, with data stored in .dat format. These raw files were converted into RINEX format using Tersus RINEX Converter, with precise start and end times for each session specified to ensure inclusion of only relevant satellite observations.

Each control point was processed under different GNSS constellation configurations using two independent software packages:

I. Tersus Geomatics Office (TGO) for high-accuracy differential processing and network adjustment.

II. RTKLIB (RTKPOST) for extracting epoch-by-epoch positional outputs under different constellation modes.

To improve the accuracy of atmospheric modeling, temperature and humidity were recorded during each observation session. These values were manually inputed into TGO to enhance tropospheric delay correction using the Saastamoinen model, a widely used empirical model that accounts for both dry and wet components of the atmosphere.

3.5.1 RINEX File Preparation

The .dat files from the receiver were converted to standard RINEX observation and navigation files using Tersus RINEX Converter. Conversion was done individually for each station, based on the specific observation start and end times recorded in the field. This ensured consistency across all datasets and eliminated unnecessary satellite data.

3.5.2 Post-Processing in Tersus Geomatics Office (TGO)

The post-processing steps followed for each control point were as follows:

1. **Import of RINEX Observation Files**

   The RINEX file for each control point was loaded into a new TGO project. Each file contained 5-seconds interval data for both pseudo-range and carrier-phase measurements.

2. **Integration of CORS Data**

   Correction data from the GeoSys CORS, time-matched to the observation session, was

added as the base station. This allowed the software to calculate a precise baseline and improve positioning through differential correction.

3. **Antenna Specifications and Height Entry**

   The correct antenna model (Tersus David30) was selected, and the measured antenna height, from the ground marker to the Antenna Reference Point (ARP), was entered for each session. This was necessary to ensure accurate elevation calculations.

4. **Data Cleaning and Signal Quality Check**

   Before baseline processing, the imported data underwent manual cleaning and inspection to remove any sources of error or signal degradation:

   Cycle slips or signal interruptions, which cause discontinuities in satellite tracking, were identified by reviewing residuals and automatically flagged or removed.

   Satellites with poor signal quality, such as those with high residual errors or low elevation angles, were excluded from processing to avoid introducing positional inaccuracies.

   The satellite observation data was visually inspected in TGO Data Plot interface, allowing for the removal of outliers and inconsistent measurements.

   This cleaning step helped improve the reliability of the computed baseline by ensuring that only high-quality, uninterrupted signals contributed to the final solution.

5. **Baseline Configuration and Processing**

   During this phase, critical settings and corrections were applied to refine the baseline solution. Environmental data temperature and humidity, recorded in the field during each session, were also entered at this stage. These values enabled the use of the Saastamoinen

model for tropospheric delay correction, improving the reliability of both horizontal and vertical positioning.

The GNSS constellation(s) to be used were selected. Each control point was reprocessed multiple times under different configurations to assess the effect of satellite geometry.

Table 3.3 Constellation Discriminant Test

Test	**Constellation(s)**
First Test	GPS
Second Test	GPS + GLONASS
Third Test	GPS + BEIDOU
Fourth Test	GLONASS + BEIDOU
Fifth Test	GPS + GLONASS + BEIDOU
Sixth Test	GLONASS
Seventh Test	BEIDOU

6. **Network Adjustment**

After the baseline between each control point and the CORS station was successfully processed, a network adjustment was performed within TGO. This step helped to fine-tune the computed position of the control point by checking for internal consistency and minimizing any small remaining errors in the baseline solution.

TGO uses adjustment algorithms to re-calculate the final position by slightly redistributing any residual errors detected in the observations. This ensures that the final coordinates are not only accurate, but also statistically reliable.

The adjustment results provided important indicators such as RMS (Root Mean Square) error values, residual. These outputs were reviewed to make sure the solution was stable and free from any significant errors that could affect the final coordinate accuracy.

In simple terms, network adjustment acts like a final quality check, tightening up the solution after processing so that the results are as precise and trustworthy as possible.

This multi-pass constellation-based post-processing strategy ensures that positional accuracy can be evaluated under controlled conditions, thereby isolating the influence of satellite geometry and constellation makeup on GNSS static survey performance.

Accuracy assessment in this study focuses on evaluating and comparing the positional quality of GNSS static solutions derived from different satellite constellation configurations. After post-processing all control points under varying constellation setups using Tersus Geomatics Office, the resulting coordinates are compared against known or reference values to assess the reliability of each solution.

3.5.3 Post-Processing in RTKLIB

In order to perform an epoch-level analysis and compare different satellite constellations, the GPS100 Control Point data was processed using RTKLIB (RTKPOST). To start, the same RINEX observation files used in the TGO software were imported into RTKPOST, along with their corresponding CORS base files. The software was configured in a static solution mode with a 10-second interval and an elevation mask of 15° to filter out low-elevation satellites. For each test, appropriate ionosphere and troposphere corrections were applied, and the satellite system settings were carefully adjusted to isolate the desired constellation or combination, such as GPS only, GPS+GLONASS, and so on. The output was specifically configured to generate epoch-by-epoch coordinates, providing the detailed position variations over time. These resulting .pos files then exported and converted to .csv files to be used for all subsequent statistical analysis, including the calculation of RMSE and CEP, and for generating the time-series plots in Python.

3.6 Accuracy Assessment

Accuracy was assessed using both absolute and relative statistical metrics. The following parameters were computed:

I. **Coordinate Differences (ΔE, ΔN, ΔH):**

These represent the difference between the processed coordinates and their known reference positions in the Easting, Northing, and Height components respectively. This metric provides a direct measure of deviation from the true location for each constellation configuration.

II. **Root Mean Square Error (RMSE):**

RMSE is calculated for each positional component (Eastings and Northings) to quantify the dispersion of errors.

The RMSE of the Eastings component is given by the formula:

$$\text{RMSE} = \sqrt{\frac{1}{n}\sum_{i=1}^{n} (E_i - E_{ref})^2} \quad (3.1)$$

The RMSE of the Northings component is given by the formula:

$$\text{RMSE} = \sqrt{\frac{1}{n}\sum_{i=1}^{n} (N_i - N_{ref})^2} \quad (3.2)$$

where E_i and N_i are the observed Eastings and Northings coordinates and E_{ref} and N_{ref} are the corresponding Eastings and Northings Coordinates of the known Control Points and n is the number of control points for TGO result analysis, while n is the number of fixed solutions (Q = 1 epochs) for RTKLIB result analysis. RMSE is computed separately for Easting and Northing.

III. Horizontal Accuracy Metrics: CEP and 2D RMS

To provide a comprehensive assessment of horizontal positional accuracy, this study incorporates the computation of Circular Error Probable (CEP) and 2D Root Mean Square (2D RMS) error for each GNSS constellation configuration. These metrics serve as statistical indicators of the dispersion and reliability of the horizontal component of the derived positions.

2D RMS represents the root sum of squares of Easting and Northing differences relative to a reference coordinate. It quantifies the average radial distance from the true point in two dimensions. CEP, on the other hand, is the radius of a circle centered at the true location within which 50% of position fixes are expected to fall, assuming a normal distribution.

The 2D RMS is computed as:

$$2DRMS = 2 \times \sqrt{(\sigma_E^2 + \sigma_N^2)} \tag{3.3}$$

$$\sigma_E = \sqrt{\frac{1}{n-1}\sum_{i=1}^{n} (\Delta E_i - \overline{\Delta E})^2} \tag{3.4}$$

$$\sigma_N = \sqrt{\frac{1}{n-1}\sum_{i=1}^{n} (\Delta N_i - \overline{\Delta N})^2} \tag{3.5}$$

The mean $\overline{\Delta E}$ and $\overline{\Delta N}$ are expressed mathematically as:

$$\overline{\Delta E} = \frac{1}{n}\sum_{i=0}^{n} \Delta E_i \tag{3.6}$$

$$\overline{\Delta N} = \frac{1}{n}\sum_{i=0}^{n} \Delta N_i \tag{3.7}$$

Where:

σ_E= standard deviation of easting value.

σ_N= standard deviation of northing value.

n = number of control points.

The Circular Error Probable (CEP) is approximated using:

$$CEP = 0.59(\sigma_x + \sigma_y) \quad (3.8)$$

These computations were performed for each processed solution (GPS-only, GPS+GLONASS, etc.) across all control stations. The results were then compared to evaluate the horizontal precision offered by each constellation combination.

The computed metrics were then used to compare each satellite constellation combination to determine which setup offers the most accurate and reliable results under the study conditions.

Graphs and charts were prepared to visually present the accuracy performance of each configuration, enabling an objective comparison.

In this study, accuracy was assessed using commonly adopted statistical measures such as Root Mean Square Error (RMSE), 2DRMS (twice the Distance Root Mean Square), and Circular Error Probable (CEP). These were computed from the Easting and Northing residuals.

CEP is a statistical measure that assumes the errors are normally distributed and equally spread in all directions. However, during the analysis, it was observed that most of the errors were tightly clustered in one direction, particularly with negative Northing values and positive Easting values. This means the error distribution was not circular but rather skewed toward one quadrant. As a result, the CEP and 2DRMS values for some constellations were extremely small.

Because CEP assumes a circular and symmetric spread of errors, its value may not fully reflect the true nature of the positional accuracy in cases like this. Even though the calculated CEP and

2DRMS are reported for consistency with GNSS standards, they should be interpreted with caution, as the distribution of errors was not uniform.

3.7 Tools and Software

To achieve high-precision static positioning and assess the effects of satellite constellation combinations, this study utilizes a combination of geodetic-grade GNSS hardware, post-processing software, correction services, and planning tools. The integration of these resources enables a complete workflow, from reliable data acquisition in the field to rigorous post-processing and accuracy evaluation. The tools were carefully selected for their ability to support multi-constellation data collection, flexible processing configurations, and detailed statistical analysis. Key components of this workflow include the Tersus David30 GNSS receiver, Tersus Geomatics Office (TGO) and RTKLIB Demo 5L, CORS correction data, Trimble GNSS Planning Online, and Microsoft Excel.

3.7.1 Tersus David30 GNSS Equipment

The primary data collection instrument is a Tersus David30 GNSS receiver, a compact palm-sized multi-constellation high-precision rover that yields centimeter-level accuracy. It is mounted on a surveyor's tribrach and tripod to record one-hour static observations at each test point. This stable setup ensures continuous, uninterrupted data capture for the duration of each static session.

3.7.2 Tersus Geomatics Office (TGO)

For post-processing, the static GNSS data were imported into Tersus Geomatics Office (TGO), a dedicated Windows application for processing Tersus receiver data. TGO supports the multi-frequency, multi-constellation static observations and allows the operator to filter which satellite systems contribute to the solution, thus enabling direct comparison between combinations of

constellations. It also integrates differential correction streams. In this project, a nearby Continuously Operating Reference Station (CORS) provided the reference data: TGO applies the CORS corrections to the rover data to perform differential processing, removing common GNSS errors. The CORS network, composed of permanent high-precision GNSS reference stations broadcasting continuous data, enables the computation of highly accurate relative positions. Using these corrections ensures that the final static positions are accurate to the centimeter level.

3.7.3 CORS Correction Service

Correction data was sourced from a Continuously Operating Reference Station (CORS) GeoSys CORS at the University of Benin. This data provides differential corrections that reduce satellite orbit and clock errors, improving the absolute positioning accuracy of the rover data.

3.7.4 Trimble GNSS Planning Online Tool

Survey planning was carried out using the Trimble GNSS Planning Online Tool, which offers sky plot visualization of satellite passes. In this web-based planner, the site coordinates are entered and a 15° elevation mask is specified to exclude low-elevation satellites. The interface also allows enabling or disabling GNSS constellations as needed. The tool then generates satellite elevation charts and a sky plot for the specified time window, verifying that a sufficient number and geometry of satellites (from GPS, GLONASS, Galileo, etc.) will be in view during the observation period.

3.7.5 Tersus RINEX Converter

The Tersus RINEX Converter is a dedicated utility provided by Tersus GNSS for converting proprietary binary observation logs from Tersus receivers into standard RINEX 2.x or 3.x formats. As stated in the release documentation, it supports output in both formats while preserving critical

metadata, such as epoch timing, multi-constellation observations, and satellite health flags, ensuring fidelity during conversion. Using this tool guarantees compatibility with post-processing software like Tersus Geomatics Office (TGO) and RTKLIB, and ensures that unique receiver metadata is accurately carried over, which is essential for high-precision static GNSS positioning.

3.7.6 Microsoft Excel

Microsoft Excel was used for coordinate analysis and visualization. The final coordinates from each processing scenario were exported to Excel, where horizontal and vertical coordinate differences were computed and summary statistics (such as root-mean-square error) were calculated. For example, the RMS error can be computed using an Excel formula. Excel's charting tools are then used to plot the results, illustrating any systematic biases or variations in precision among the different constellation configurations. Overall, Excel serves as the final analysis stage in the workflow, allowing quick computation of error metrics and clear graphical presentation of the positioning accuracy results.

3.7.7 Tersus MergeRinexFiles Tool

The MergeRinexFiles Tool, provided by Tersus GNSS, enables seamless concatenation of RINEX files that cover adjacent time intervals. Many GNSS reference stations, including CORS networks, provide observation data in fixed-duration segments, commonly one or two hour files, to simplify data handling and distribution. When a static GNSS session overlaps two such segments, as may happen with one-hour rover sessions beginning toward the end of the first file, merging is essential to maintain continuous observation records. The MergeRinexFiles Tool processes these files by combining headers and observation data while preserving epoch sequence and metadata integrity. The resulting merged file aligns perfectly with the rover's session duration, ensuring uninterrupted

data coverage for baseline processing in Tersus Geomatics Office. This continuity is critical to avoid gaps that could disrupt differential processing and degrade positional accuracy.

3.3.8 RTKLIB Demo5L

RTKLIB Demo5L served as the primary software for processing the raw GNSS observation data. This open-source software was used to perform post-processing of the static GNSS data to derive precise positional coordinates for GPS100 control point. It allowed for the configuration of various processing parameters, including the selection of satellite constellations (GPS, GLONASS, BEIDOU), the data quality flag (Q=1 for fixed solutions), and the observation interval. The output of RTKLIB provided the detailed epoch-by-epoch positional solutions that were used for subsequent analysis.

3.3.9 Python

Python, leveraging powerful data science libraries like pandas and matplotlib, was an essential tool for the analysis and visualization phase of this study. The software was utilized to import the processed data from RTKLIB, enabling a strong platform for computing various statistical metrics. It was used to calculate not only classical parameters such as the mean, standard deviation, and RMSE but also more robust measures like the median and the Median Absolute Deviation (MAD), which were particularly important for interpreting the accuracy of the non-normally distributed datasets. Furthermore, Python was instrumental in generating the time-series plots that provided a critical visual understanding of the solution's stability over the observation period.

3.3.10 ArcGIS

ArcGIS served a specific and crucial role in the workflow of this project: the conversion of coordinates. The software was used to transform the latitude and longitude coordinates derived

from RTKLIB's post-processing into the appropriate WGS UTM Zone 31N projected coordinate system. This step was necessary to ensure that all data was in a uniform system, allowing for accurate calculations and a consistent basis for analyzing the positional errors in the Easting and Northing components.

3.8 Limitations of the Methodology

Although the methodology adopted in this study is designed to ensure accurate and reliable assessment of GNSS static positioning, certain limitations remain. One of the primary constraints is the reliance on a single brand and model of GNSS receiver (Tersus David30), which may influence satellite tracking capability and processing compatibility compared to other high-end geodetic receivers. Additionally, the observation sessions are limited to approximately one hour per point, which while generally sufficient may not fully capture long-term satellite geometry variations, multipath effects, or atmospheric changes.

The use of a single nearby CORS for correction limits the evaluation to a fixed baseline configuration. Variations in baseline length or reference station geometry were not explored.

Finally, local environmental conditions such as tree cover, buildings, and atmospheric interference although minimized through survey planning may still introduce noise or reduce satellite visibility during some sessions. These factors are taken into account during interpretation but cannot be entirely eliminated.

CHAPTER FOUR

RESULT AND DISCUSSIONS

4.1 TGO Processed Coordinate Results per Constellation

The results of the static GNSS post-processing under different satellite constellation combinations are presented below. Each control station was processed using Tersus Geomatics Office. The configurations analyzed include GPS-only, GPS+GLONASS, GPS+BEIDOU, GLONASS+BEIDOU, BEIDOU only, GLONASS only and the combined GPS+GLONASS+BEIDOU setup.

The processed coordinates, Easting (E), Northing (N), and Height (H) for each station under the various constellation setups are as follows:

GPS + GLONASS + BEIDOU

Station	Eastings (E)	Northings (N)	Height (H)
RaphUNB02	789804.4759	708399.1183	121.8381
RaphUNB01	789774.3027	708303.6179	122.2193
UNIBEN02	789875.7757	708645.3647	120.3146
UNIBEN01	789633.1238	708611.8798	125.0994
GPS100	789398.0531	708576.2219	128.4651

GPS + GLONASS

Station	Eastings (E)	Northings (N)	Height (H)
RaphUNB02	789804.4689	708399.1310	121.8603
RaphUNB01	789774.2956	708303.6450	122.2184
UNIBEN02	789875.7634	708645.3653	120.3136
UNIBEN01	789633.1282	708611.8887	125.1186
GPS100	789398.0542	708576.2251	128.4840

GPS + BEIDOU

Station	Eastings (E)	Northings (N)	Height (H)
RaphUNB02	789804.4750	708399.1316	121.8617
RaphUNB01	789774.3003	708303.6196	122.2138
UNIBEN02	789875.7757	708645.3647	120.3146
UNIBEN01	789633.1229	708611.8768	125.0992
GPS100	789398.0533	708576.2225	128.4625

GLONASS + BEIDOU

Station	Eastings (E)	Northings (N)	Height (H)
RaphUNB02	789804.4781	708399.1262	121.8494
RaphUNB01	789774.3075	708303.6479	122.2933
UNIBEN02	789875.7642	708645.3767	120.3247
UNIBEN01	789633.6171	708612.0944	125.1070
GPS100	789398.0553	708576.2228	128.4692

GPS

Station	Eastings (E)	Northings (N)	Height (H)
RaphUNB02	789804.4689	708399.1310	121.8603
RaphUNB01	789774.2846	708303.6493	122.2388
UNIBEN02	789875.7759	708645.3624	120.3114
UNIBEN01	789633.1310	708611.8848	125.1284
GPS100	789398.0488	708576.2312	128.5018

GLONASS

Station	Eastings (E)	Northings (N)	Height (H)
RaphUNB02	789804.4821	708399.0723	121.9689
RaphUNB01	789774.3084	708303.6543	122.2889
UNIBEN02	789875.7800	708645.4167	119.3393
UNIBEN01	789633.2645	708611.9255	125.1398
GPS100	789398.0526	708576.2248	128.4767

BEIDOU

Station	Eastings (E)	Northings (N)	Height (H)
RaphUNB02	789804.4796	708399.1274	121.8665
RaphUNB01	789774.3143	708303.6396	122.2647
UNIBEN02	789875.7637	708645.3779	119.3248
UNIBEN01	789633.6042	708612.0944	125.1171
GPS100	789397.9202	708576.3487	128.3551

4.2 TGO Positional Accuracy Assessment

This study assessed horizontal positional accuracy using statistical metrics derived from differences between the processed coordinates and their known ground truth values. For each satellite constellation combination (GPS-only, GPS+GLONASS, GPS+BEIDOU, GLONASS+BEIDOU, GPS+GLONASS+BEIDOU, GLONASS, and BEIDOU), the coordinate errors in Easting (ΔE) and Northing (ΔN) were calculated as:

$$\Delta E_i = E_i - E_{ref} \tag{4.1}$$

$$\Delta N_i = N_i - N_{ref} \tag{4.2}$$

From these coordinate differences, the Root Mean Square Error (RMSE) was computed separately for Eastings and Northings using the formulas:

The RMSE of the Eastings component is given by the formula:

$$\text{RMSE} = \sqrt{\frac{1}{n}\sum_{i=1}^{n} (E_i - E_{ref})^2} \tag{4.3}$$

The RMSE of the Northings component is given by the formula:

$$\text{RMSE} = \sqrt{\frac{1}{n}\sum_{i=1}^{n} (N_i - N_{ref})^2} \tag{4.4}$$

This metric represents the average magnitude of the positional error across all stations for each constellation.

Across the five control points, the mean of these errors was computed as:

$$\overline{\Delta E} = \frac{1}{n}\sum_{i=0}^{n} \Delta E_i \tag{4.5}$$

$$\overline{\Delta N} = \frac{1}{n}\sum_{i=0}^{n} \Delta N_i \tag{4.6}$$

The standard deviations of the Easting and Northing components were calculated using:

$$\sigma_E = \sqrt{\frac{1}{n-1}\sum_{i=1}^{n} (\Delta E_i - \overline{\Delta E})^2} \tag{4.7}$$

$$\sigma_N = \sqrt{\frac{1}{n-1}\sum_{i=1}^{n} (\Delta N_i - \overline{\Delta N})^2} \tag{4.8}$$

The parameters are defined as:

ΔE_i and ΔN_i are the coordinate difference between the processed and known coordinate at the ith station.

E_i and N_i are the Eastings and Northings processed coordinates at the ith station.

E_{ref} and N_{ref}, are the Eastings and Northings reference/known coordinates.

$\overline{\Delta E}$ and $\overline{\Delta N}$ represents the mean of Eastings and Northings error for each constellation across the five control points.

σ_E and σ_N are standard deviations of Eastings and Northings errors for each constellation across the five control points.

n is number of control points.

These values help quantify the spread or variation of horizontal errors in each direction.

The results for ΔE_i and ΔN_i for each constellation across the five control stations is given in the table below:

GPS						
Station	**E_{ref}**	**N_{ref}**	**E_i**	**N_i**	**ΔE_i**	**ΔN_i**
RaphUNB02	789804.4312	708399.3471	789804.4689	708399.131	0.0377	-0.2161
RaphUNB01	789774.1402	708303.8314	789774.2846	708303.6493	0.1444	-0.1821
UNIBEN02	789875.7324	708645.7109	789875.7759	708645.3624	0.0435	-0.3485
UNIBEN01	789633.0081	708612.0767	789633.131	708611.8848	0.1229	-0.1919
GPS100	789397.9902	708576.4309	789398.0488	708576.2312	0.0586	-0.1997

GLONASS						
Station	**E_{ref}**	**N_{ref}**	**E_i**	**N_i**	**ΔE_i**	**ΔN_i**
RaphUNB02	789804.4312	708399.3471	789804.4821	708399.0723	0.0509	-0.2748
RaphUNB01	789774.1402	708303.8314	789774.3084	708303.6543	0.1682	-0.1771
UNIBEN02	789875.7324	708645.7109	789875.7800	708645.4167	0.0476	-0.2942
UNIBEN01	789633.0081	708612.0767	789633.2645	708611.9255	0.2564	-0.1512
GPS100	789397.9902	708576.4309	789398.0526	708576.2248	0.0624	-0.2061

BEIDOU						
Station	**E_{ref}**	**N_{ref}**	**E_i**	**N_i**	**ΔE_i**	**ΔN_i**
RaphUNB02	789804.4312	708399.3471	789804.4796	708399.1274	0.0484	-0.2197
RaphUNB01	789774.1402	708303.8314	789774.3143	708303.6396	0.1741	-0.1918
UNIBEN02	789875.7324	708645.7109	789875.7637	708645.3779	0.0313	-0.333
UNIBEN01	789633.0081	708612.0767	789633.6042	708612.0944	0.5961	0.0177
GPS100	789397.9902	708576.4309	789397.9202	708576.3487	-0.07	-0.0822

GPS + GLONASS						
Station	**E_{ref}**	**N_{ref}**	**E_i**	**N_i**	**ΔE_i**	**ΔN_i**
RaphUNB02	789804.4312	708399.3471	789804.4689	708399.131	0.0377	-0.2161
RaphUNB01	789774.1402	708303.8314	789774.2956	708303.645	0.1554	-0.1864
UNIBEN02	789875.7324	708645.7109	789875.7634	708645.3653	0.031	-0.3456
UNIBEN01	789633.0081	708612.0767	789633.1282	708611.8887	0.1201	-0.188
GPS100	789397.9902	708576.4309	789398.0542	708576.2251	0.064	-0.2058

GPS + BEIDOU						
Station	**E_{ref}**	**N_{ref}**	**E_i**	**N_i**	**ΔE_i**	**ΔN_i**
RaphUNB02	789804.4312	708399.3471	789804.475	708399.1316	0.0438	-0.2155
RaphUNB01	789774.1402	708303.8314	789774.3003	708303.6196	0.1601	-0.2118
UNIBEN02	789875.7324	708645.7109	789875.7757	708645.3647	0.0433	-0.3462
UNIBEN01	789633.0081	708612.0767	789633.1229	708611.8768	0.1148	-0.1999
GPS100	789397.9902	708576.4309	789398.0533	708576.2225	0.0631	-0.2084

GLONASS + BEIDOU						
Station	**E_{ref}**	**N_{ref}**	**E_i**	**N_i**	**ΔE_i**	**ΔN_i**
RaphUNB02	789804.4312	708399.3471	789804.4781	708399.1262	0.0469	-0.2209
RaphUNB01	789774.1402	708303.8314	789774.3075	708303.6479	0.1673	-0.1835
UNIBEN02	789875.7324	708645.7109	789875.7642	708645.3767	0.0318	-0.3342
UNIBEN01	789633.0081	708612.0767	789633.6171	708612.0944	0.609	0.0177
GPS100	789397.9902	708576.4309	789398.0553	708576.2228	0.0651	-0.2081

GPS+ GLONASS + BEIDOU						
Station	**E_{ref}**	**N_{ref}**	**E_i**	**N_i**	**ΔE_i**	**ΔN_i**
RaphUNB02	789804.4312	708399.3471	789804.4759	708399.1183	0.0447	-0.2288
RaphUNB01	789774.1402	708303.8314	789774.3027	708303.6179	0.1625	-0.2135
UNIBEN02	789875.7324	708645.7109	789875.7757	708645.3647	0.0433	-0.3462
UNIBEN01	789633.0081	708612.0767	789633.1238	708611.8798	0.1157	-0.1969
GPS100	789397.9902	708576.4309	789398.0531	708576.2219	0.0629	-0.209

Constellation	Mean ΔE	Mean ΔN	σ_E	σ_N	RMSE (E)	RMSE (N)
GPS	0.08142	-0.22766	0.04888	0.06869	0.09242	0.235804
GPS+GLONASS	0.08164	-0.22838	0.054143	0.0667	0.094923	0.236043
GPS+BEIDOU	0.08502	-0.23636	0.051098	0.06167	0.096526	0.242712
GLONASS+BEIDOU	0.18402	-0.1858	0.243414	0.12764	0.285068	0.218072
GPS+GLO+BEIDOU	0.08582	-0.23888	0.051954	0.06107	0.097593	0.245046
GLONASS	0.1171	-0.22068	0.092494	0.06179	0.143375	0.227496
BEIDOU	0.15598	-0.1618	0.260873	0.13427	0.280666	0.201502

4.2.1 CEP and 2D RMS Computation

To further summarize positional performance, the Circular Error Probable (CEP) and Two-Dimensional Root Mean Square (2D RMS) error were computed as:

The 2D RMS is computed as:

$$2DRMS = 2 \times \sqrt{(\sigma_E^2 + \sigma_N^2)} \quad (4.9)$$

The Circular Error Probable (CEP) is approximated using:

$$\text{CEP} = 0.59(\sigma_E + \sigma_N) \quad (4.10)$$

Theoretically, CEP gives the radius within which approximately 50% of the horizontal position errors fall, and 2D RMS approximates the radius containing about 95% of the errors.

These formulas were applied to all coordinate differences grouped by constellation configuration. This approach allows each configuration to be evaluated statistically across all the control points.

The resulting statistics for each satellite combination are presented in the table below. These values were computed using the above formulas and provide a comprehensive comparison of each configuration's horizontal positioning performance.

Note that the CEP and 2DRMS assumes the errors are normally distributed.

The results for the mean, standard deviation, CEP and 2DRMS for each constellation across the five control points is given in the table below:

Constellation	Mean ΔE	Mean ΔN	σ_E	σ_N	2D RMS	CEP
GPS	0.08142	-0.22766	0.04888	0.06869	0.16861	0.06937
GPS+GLONASS	0.08164	-0.22838	0.054143	0.0667	0.17181	0.0713
GPS+BEIDOU	0.08502	-0.23636	0.051098	0.06167	0.16018	0.06653
GLONASS+BEIDOU	0.18402	-0.1858	0.243414	0.12764	0.5497	0.21892
GPS+GLO+BEIDOU	0.08582	-0.23888	0.051954	0.06107	0.16036	0.06668
GLONASS	0.1171	-0.22068	0.092494	0.06179	0.22247	0.09103
BEIDOU	0.15598	-0.1618	0.260873	0.13427	0.5868	0.23314

It is important to note that the parameters analyzed including Mean Error, RMSE, 2DRMS, and CEP, were derived from measurements collected across these five stations. While this approach provides comparative insight into constellation performance, the relatively small spatial extent and controlled observation conditions impose certain limitations. Environmental variability, satellite geometry, and correction service availability may differ in other settings, potentially affecting result generalizability

4.2.2 Interpretation of Positioning Accuracy Across All Stations

The statistical parameters, including mean horizontal errors (ΔE and ΔN), standard deviations, root mean square errors (RMSE), circular error probable (CEP), and twice the distance root mean square (2DRMS), were computed by aggregating the positioning results from five independent control stations. Each station was observed using varying satellite constellation configurations to assess the consistency and reliability of the solutions.

Across all configurations, results clearly show that solutions incorporating the GPS constellation consistently outperformed others in terms of both accuracy and precision. Notably, the

GPS+BEIDOU combination exhibited the lowest 2DRMS (0.1602 m) and CEP (0.0665 m), indicating superior horizontal positioning performance when evaluated across all stations. Similarly, GPS-only and GPS+GLONASS+BEIDOU configurations yielded comparably strong results, with relatively low mean errors and dispersion in both the Easting and Northing components.

In contrast, constellation combinations excluding GPS, particularly BEIDOU-only and GLONASS+BEIDOU, displayed significantly poorer performance across the five stations. BEIDOU-only, for instance, recorded the highest 2DRMS (0.5868 m) and CEP (0.2331 m), alongside large standard deviations in both components, suggesting a less stable and less accurate solution. Although the GLONASS-only solution performed better than BEIDOU-only, it still lagged behind configurations involving GPS.

These findings emphasize the central importance of GPS in achieving robust and precise positioning. While additional constellations such as GLONASS and BEIDOU can serve as useful augmentations, their standalone performance, as observed across multiple control stations, is insufficient for high-accuracy GNSS applications. The results also suggest that integrated GNSS solutions are most effective when GPS forms the foundational constellation, complemented by others only where beneficial satellite geometry or redundancy is required.

4.2.3 Limitations of TGO Result

It is important to note that the positioning performance evaluated in this analysis is based on data collected from only five control stations within a specific geographic area. The results may not fully capture the variability of GNSS performance in different environmental or satellite visibility conditions. Additionally, disparities in satellite geometry, signal multipath, and correction

availability (particularly for standalone BEIDOU and GLONASS solutions) may have influenced the observed accuracy. These factors should be considered when generalizing the findings beyond the current study context.

4.2.4 Visualization of TGO Result

To better illustrate the spread and concentration of positional errors, a scatter plot of ΔE (Eastings error) against ΔN (Northings error) was generated for each satellite constellation configuration across all five control points. Each point on the plot represents a horizontal error vector from the known control point position.

This visualization helps in identifying both the bias and dispersion of position estimates. Configurations with tightly clustered points near the origin indicate higher positional consistency and accuracy.

A bar chart was generated for to visualize statistical metrics such as RMSE, 2DRMS and CEP.

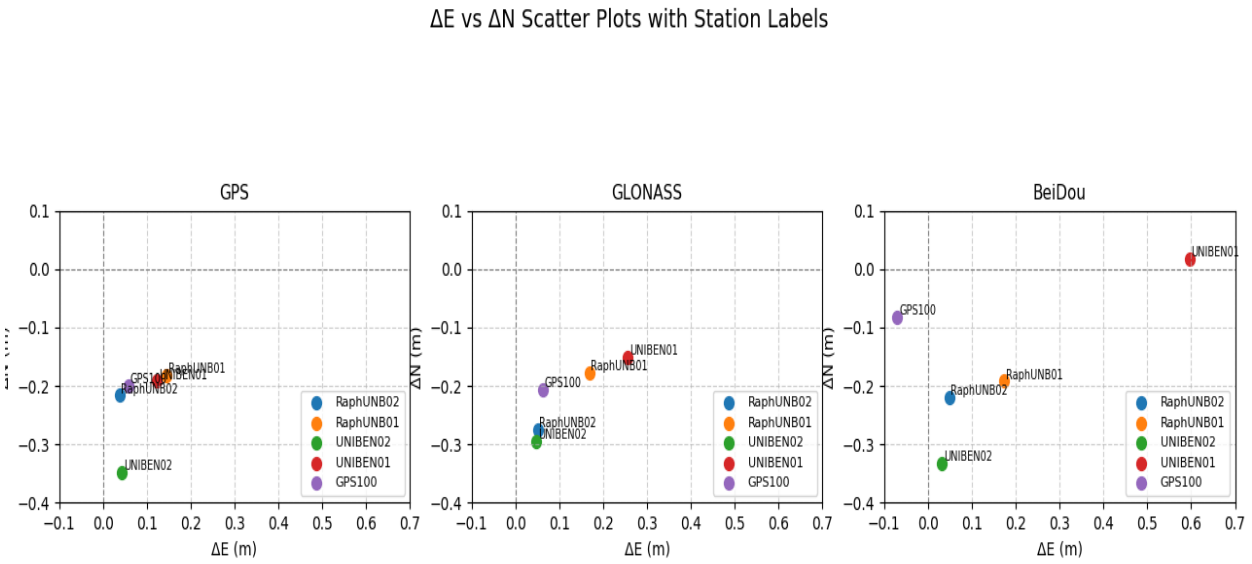

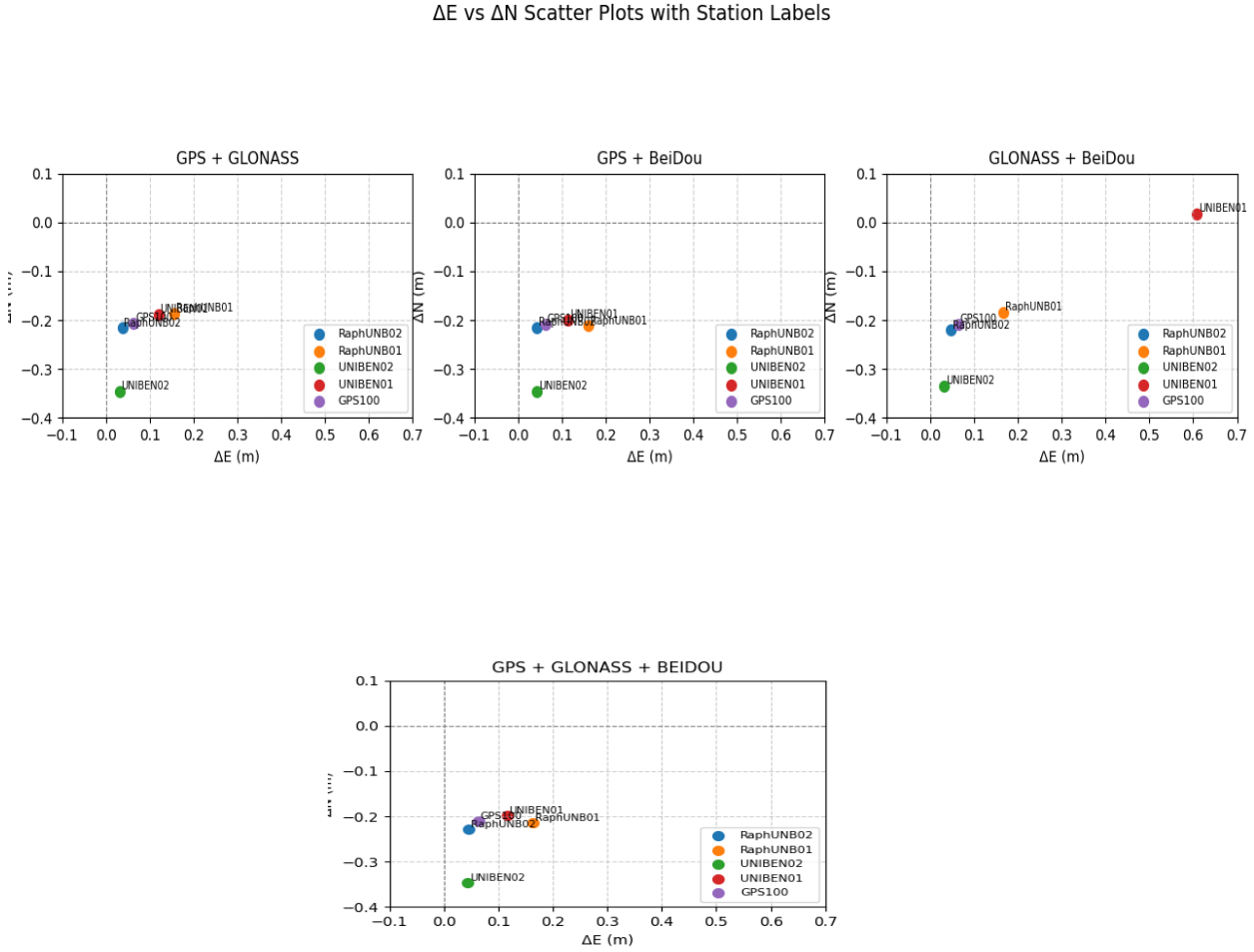

Figure 4.1: Northings and Eastings Errors Scatter Plots

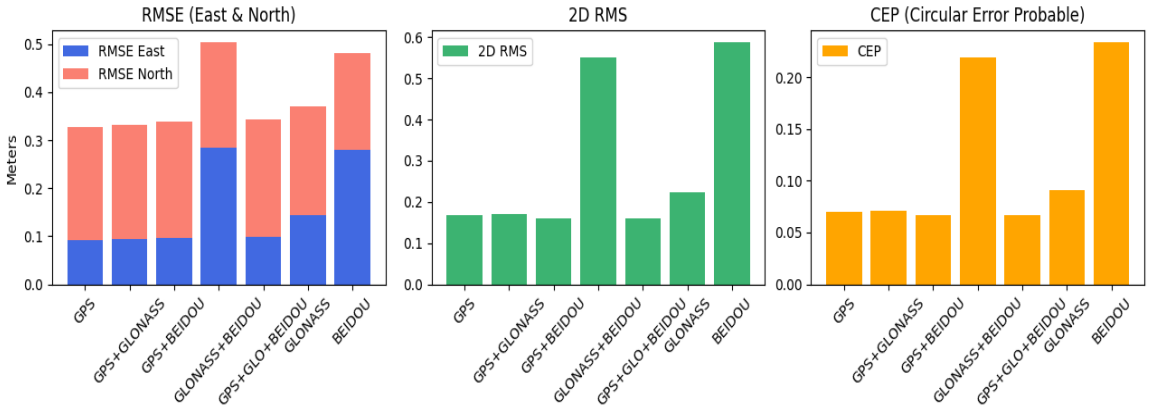

Figure 4.2: RMSE, 2D RMS and CEP Plots

4.3 RTKLIB Positioning Results

This section presents the results obtained from the RTKLIB post-processing of the GPS100 control point using different satellite constellations. RTKLIB outputs coordinate solutions at a regular epoch interval of 10 seconds, allowing for a time-series evaluation of positioning accuracy.

Single and combined constellation was processed, and the resulting Easting (E), Northing (N), and Height (H) coordinates were compared to the known GPS100 control point coordinates. The coordinate differences (ΔE, ΔN, ΔH) were computed for each epoch to evaluate positioning errors.

For each constellation, the following statistical values were computed:

I. Mean error in ΔE and ΔN defined by equation 4.5 and 4.6,

II. Standard deviation defined by equation 4.7 and 4.8,

III. Root Mean Square Error (RMSE) defined by equation 4.3 and 4.4,

IV. Circular Error Probable (CEP) defined by equation 4.9,

V. 2D Root Mean Square (2DRMS) defined by equation 4.10

VI. Median Absolute Deviation (MAD), defined by equation 4.11, 4.12 and 4.13

Where, n in equation 4.3, 4.4, 4.5, 4.6, 4.7 and 4.8 is the number of fixed (Q = 1) epochs for this analysis.

The median and the median Absolute Deviation is described by the formulas:

$$M = X_{\frac{(n+1)}{2}} \text{ if n is odd} \qquad 4.11$$

$$M = \frac{(X_{\frac{n}{2}} + X_{\frac{n}{2+1}})}{2} \text{ if n is even} \qquad 4.12$$

Where, M is the median, x is the sorted dataset (ΔE and ΔN), n is the total number of data points (number of Q = 1 epochs).

$$\text{MAD} = \text{median}(|x_i - M|) \quad 4.13$$

Where, x_i is each data point (ΔE and ΔN), M is the median and $|x_i - M|$ is the absolute difference of each data point from the median.

4.3.1 Normality Assessment of RTKLIB Residuals

Before deciding which statistical measures were most appropriate, a normality test was performed on the error values obtained from RTKLIB. The Shapiro-Wilk test was applied to the ΔE and ΔN values for each constellation to determine whether the data followed a normal distribution.

This test is important because traditional metrics like the mean and standard deviation are most meaningful when the data follows a normal distribution. While RMSE can be computed regardless of distribution, it is sensitive to outliers and may not reflect typical performance in non-normal datasets. Therefore, when the data is not normally distributed, robust statistics such as the median and Median Absolute Deviation (MAD) offer more reliable insights.

The Shapiro-Wilk test is based on the formula:

$$W = \frac{(\sum_i^n a_i x_{(i)})^2}{\sum_i^n (x_i - \bar{x})^2} \quad 4.14$$

Where, $x_{(i)}$ represents the i-th ordered observation of the sample, $\bar{x}$ is the sample mean and a_i are coefficients calculated from the expected values of the order statistics of a standard normal distribution and their covariance matrix.

The result of the normality tests is given in the table below:

Table 4.1 Normality tests results

Constellation	Shapiro p (ΔE)	Normality (ΔE)	Shapiro p (ΔN)	Normality(ΔN)
G	2.42×10^{-7}	Not normal	6.95×10^{-11}	Not normal
R	3.70×10^{-25}	Not normal	5.26×10^{-25}	Not normal
C	7.28×10^{-5}	Not normal	$5.62e\times10^{-6}$	Not normal
GR	1.96×10^{-25}	Not normal	$8.13e\times10^{-26}$	Not normal
GC	1.22×10^{-7}	Not normal	3.47×10^{-9}	Not normal
RC	7.28×10^{-5}	Not normal	5.62×10^{-6}	Not normal
GRC	6.22×10^{-7}	Not normal	4.17×10^{-9}	Not normal

Where, G, R, C, GR, GC, RC and GRC represent GPS, GLONASS, BEIDOU, GPS+GLONASS, GPS+BEIDOU, GLONASS+BEIDOU and GPS+GLONASS+BEIDOU constellation(s) respectively.

If the p-value is less than 0.05, it suggests the data is not normally distributed at the 5% significance level.

Based on these results, robust statistical measures such as the Median and MAD were used alongside classical metrics for a more reliable evaluation of horizontal accuracy.

To better understand the distribution of the coordinate errors from the RTKLIB epoch-based results, Kernel Density Estimate (KDE) plots were generated for the ΔE (East error), and ΔN (North error). These plots allow for a visual inspection of the spread and shape of the Eastings and Northings errors.

The KDE plots provide a smoothed version a histogram, which helps reveal patterns or deviations from normal distribution, such as skewness or multi-modality.

4.3.2 Visual Assessment of Normality Using Q-Q Plots

Q-Q plots were used to assess the normality of the ΔE and ΔN residuals by comparing their quantiles to those of a standard normal distribution. The plots revealed clear deviations from the reference line, especially in the tails, indicating heavy-tailed and asymmetric distributions. These observations align with the histogram, KDE, and Shapiro-Wilk test results, further confirming non-normality.

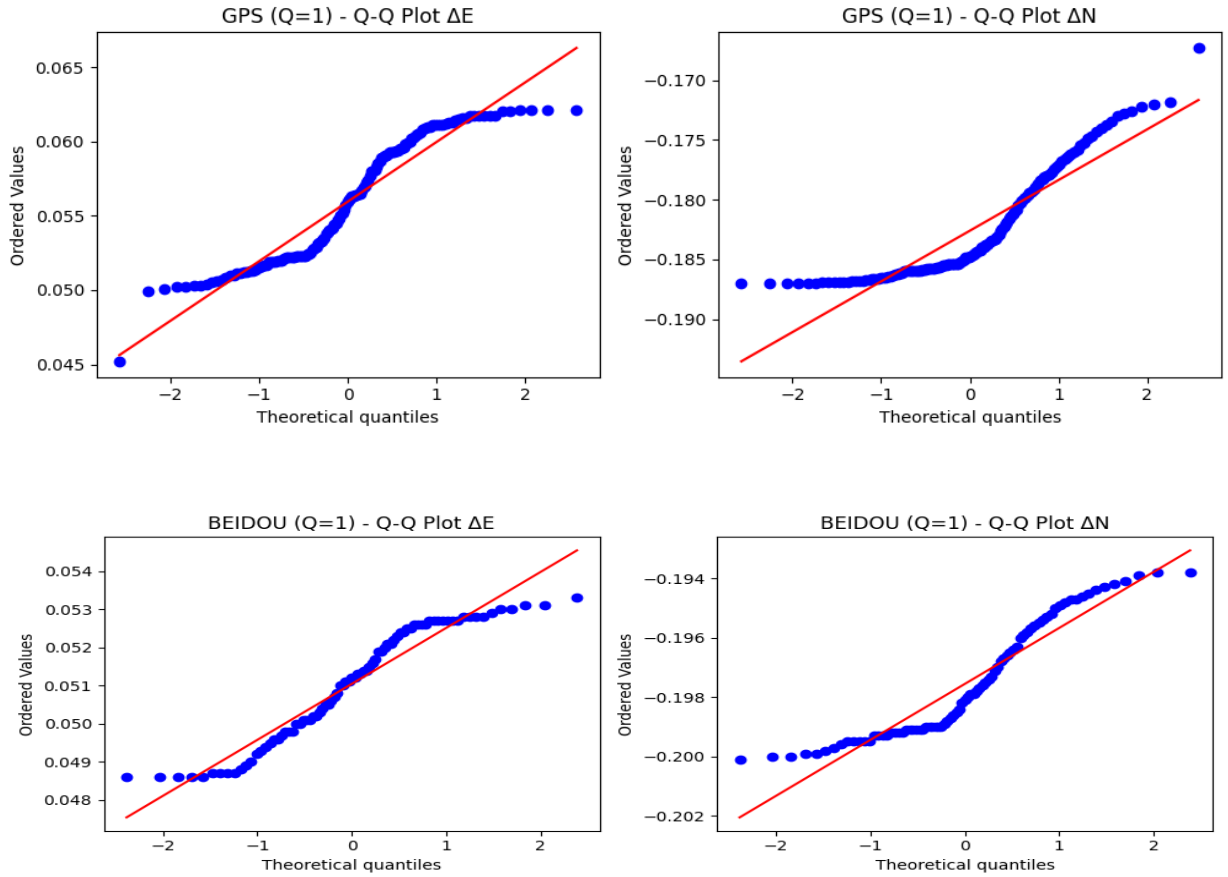

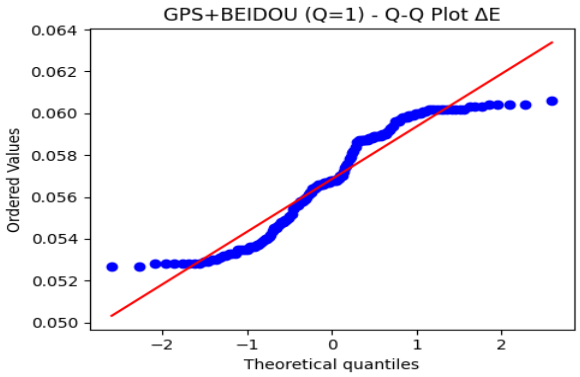
GPS+BEIDOU (Q=1) - Q-Q Plot ΔE
Ordered Values
Theoretical quantiles

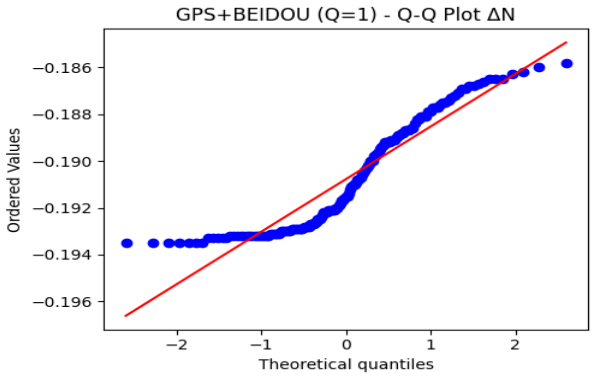
GPS+BEIDOU (Q=1) - Q-Q Plot ΔN
Ordered Values
Theoretical quantiles

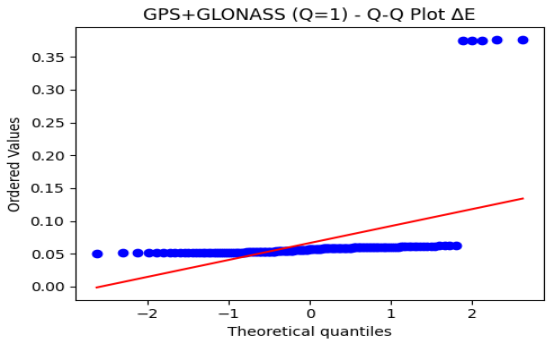
GPS+GLONASS (Q=1) - Q-Q Plot ΔE
Ordered Values
Theoretical quantiles

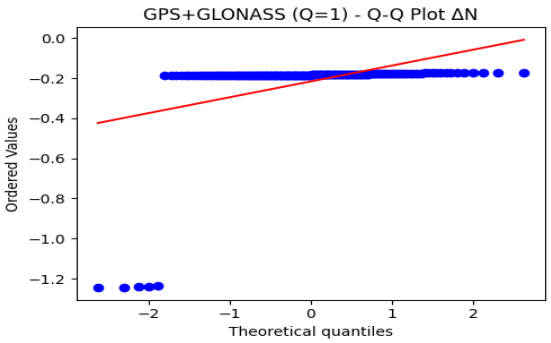
GPS+GLONASS (Q=1) - Q-Q Plot ΔN
Ordered Values
Theoretical quantiles

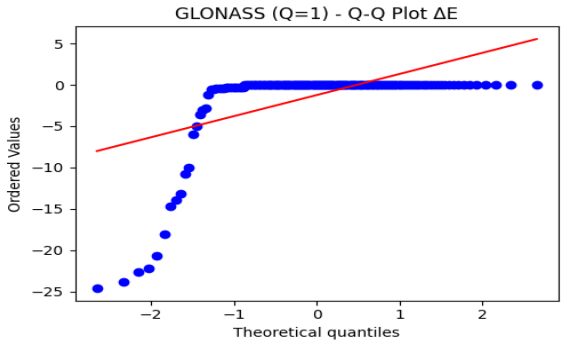
GLONASS (Q=1) - Q-Q Plot ΔE
Ordered Values
Theoretical quantiles

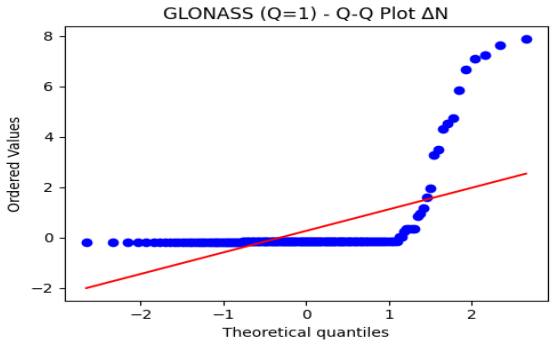
GLONASS (Q=1) - Q-Q Plot ΔN
Ordered Values
Theoretical quantiles

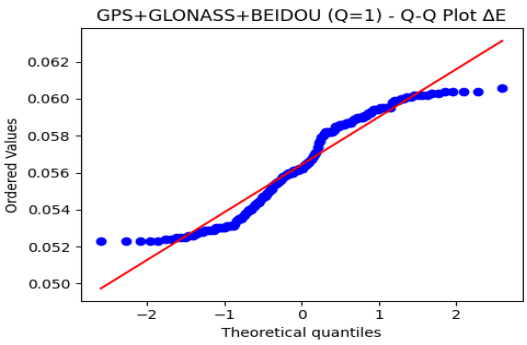
GPS+GLONASS+BEIDOU (Q=1) - Q-Q Plot ΔE
Ordered Values
Theoretical quantiles

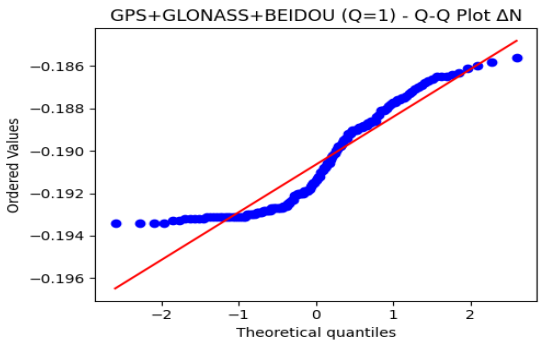
GPS+GLONASS+BEIDOU (Q=1) - Q-Q Plot ΔN
Ordered Values
Theoretical quantiles

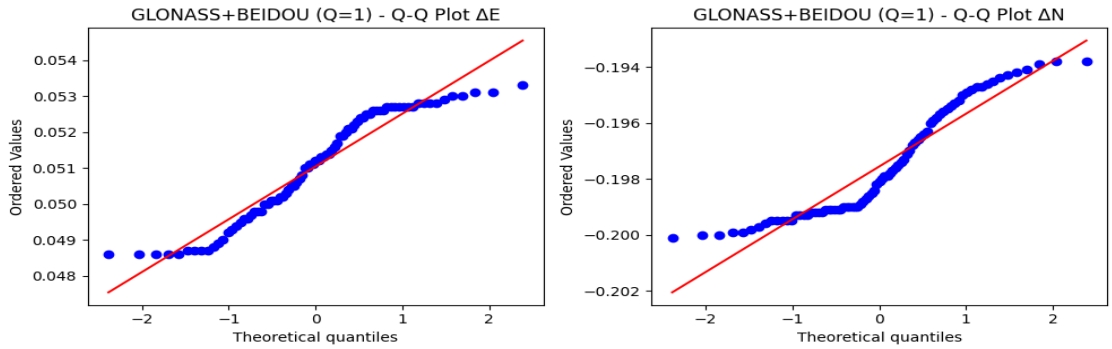

Figure 4.3: Kernel Density Estimate (KDE) Plots

From these plots, it was observed that the error distributions were not symmetric and did not follow the bell-shaped curve typical of a normal distribution. This aligns with the results from the Shapiro-Wilk normality tests, which confirmed that the error distributions deviate significantly from normality.

Therefore, in the following sections, robust statistics such as median, Median Absolute Deviation (MAD), and percentile-based CEP and 2DRMS were used for error analysis instead of relying solely on mean-based metrics.

4.3.3 Analyzing RTKPOST Epoch-Based Solutions

This section presents a detailed summary of the analysis of epoch-based solutions derived from RTKPOST, of GPS100 control point. The objective was to evaluate the positional accuracy of these solutions over a 10-second observation period. To achieve this, a range of statistical parameters were computed, including the mean and RMSE, as well as both classical and robust statistical measures. The inclusion of robust statistical methods is particularly important for this analysis, as it mitigates the influence of potential outliers in the data, thereby providing a more reliable and stable assessment of the solution's precision and accuracy.

The RMSE, classical and robust statistical parameter computer for GPS100 at 10-seconds epochs for Q = 1 solutions is given by the tables below:

Constellations	**Mean ΔE**	**Mean ΔN**	**Mean ΔH**	$\boldsymbol{\sigma_E}$	$\boldsymbol{\sigma_N}$	$\boldsymbol{\sigma_H}$
GPS+GLONASS+BEIDOU	0.056436	-0.19065	1.463739	0.002641	0.00235	0.001898
GPS+GLONASS	0.066422	-0.21623	1.513071	0.056328	0.186458	0.142679
GPS+BEIDOU	0.056852	-0.19077	1.463054	0.002587	0.002351	0.00192
GLONASS+BEIDOU	0.051046	-0.19755	1.44606	0.001495	0.001947	0.000618
GPS	0.055955	-0.18259	1.489004	0.004137	0.004566	0.007512
GLONASS	-1.23649	0.264699	3.135236	4.536972	1.496876	5.878875
BEIDOU	0.051046	-0.19755	1.44606	0.001495	0.001947	0.000618

Constellations	**RMSE (E)**	**RMSE (N)**	**RMSE (H)**	**CEP**	**2DRMS**
GPS+GLONASS+BEIDOU	0.056497	0.190661	1.463741	0.002944	0.00707
GPS+GLONASS	0.086974	0.285132	1.519741	0.143243	0.389561
GPS+BEIDOU	0.056911	0.190789	1.463056	0.002913	0.006991
GLONASS+BEIDOU	0.051067	0.197564	1.446061	0.002031	0.004909
GPS	0.056107	0.182647	1.489023	0.005135	0.012323
GLONASS	4.689854	1.515858	6.647725	3.55997	9.555051
BEIDOU	0.051067	0.197564	1.446061	0.002031	0.004909

Constellations	**Median(ΔE)**	**Median(ΔN)**	**MAD(ΔE)**	**MAD(ΔN)**
GPS+GLONASS+BEIDOU	0.0562	-0.1914	0.0025	0.0017
GPS+GLONASS	0.0565	-0.1844	0.0037	0.0022
GPS+BEIDOU	0.0568	-0.1915	0.0023	0.0017
GLONASS+BEIDOU	0.0512	-0.1981	0.0014	0.0014
GPS	0.056	-0.18475	0.0038	0.0019
GLONASS	0.05244	-0.15801	0.001847	0.007588
BEIDOU	0.0512	-0.1981	0.0014	0.0014

The analysis of the processed GNSS data reveals a clear and consistent pattern, multi-constellation solutions provide a significant improvement in positional accuracy and precision over single-

constellation solutions. The combined GPS+GLONASS+BEIDOU configuration, for example, demonstrated better performance with a horizontal bias of 0.056436 m in Easting and −0.19065 m in Northing, and very low standard deviations (σ_E = 0.002641m and σ_N = 0.00235m). This high level of precision was also observed in other combinations, such as GPS+BEIDOU and GLONASS+BEIDOU.

Among the single constellations, both GPS and BEIDOU provided highly reliable data, though with a consistent horizontal bias similar to the combined solutions. The BEIDOU single solution was particularly precise, achieving standard deviations (σ_E =0.002476m and σ_N=0.002242m) that were comparable to those of the multi-constellation solutions.

In stark contrast, the single GLONASS solution performed poorly, displaying a large and inconsistent bias with Mean ΔE of −1.23649m and Mean ΔN of 0.264699m. Its classical error metrics were severely degraded by a large spread of data, as seen in the high standard deviation values (σ_E = 4.536972m and σ_N = 1.496876m).

The distinction between classical and robust statistical parameters proved critical for a complete interpretation. For the stable solutions like GPS+GLONASS+BEIDOU, the standard deviation was very close to the Median Absolute Deviation (MAD(ΔE) = 0.0025m), indicating a tight distribution of errors. However, for the unstable GLONASS data, there was a significant difference between the high standard deviation (σ_E = 4.536972m) and the much smaller MAD (MAD(ΔE) = 0.001847 m). This disparity clearly confirms the presence of significant outliers in the GLONASS data, which inflate classical metrics but are appropriately ignored by the robust MAD, providing a more truthful measure of the solution's central tendency and spread.

4.4 Time Series Analysis of Positional Error

To assess the consistency and stability of GNSS positioning solutions, positional errors were analyzed with respect to time. This section presents the variation of Eastings, Northings, Height, 2D Error, and number of satellites across the observation epochs for different constellations: GPS, GLONASS, BeiDou, GPS+GLONASS, GPS+BEIDOU, GLONASS+BEIDOU, GPS+GLONASS+BEIDOU.

4.4.1 Easting Errors Over Time

The time-series graphs for Easting errors reveal three distinct behaviors. Most multi-constellation solutions, including GPS+GLONASS+BEIDOU, GLONASS+BEIDOU, and GPS+BEIDOU, along with the standalone BEIDOU solution, are highly stable, with errors remaining within a narrow, predictable band (between 0.05 and 0.06 meters). In sharp contrast, the standalone GLONASS solution is extremely unstable, with its error dramatically plummeting to around -25 meters over time. Finally, both the standalone GPS and the GPS+GLONASS solutions show a delayed breakdown, where the error remains stable for a while before suddenly spiking upwards.

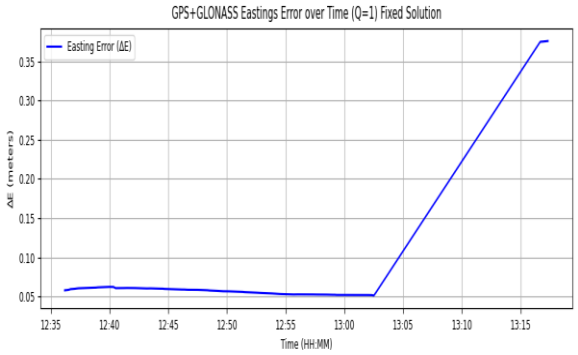

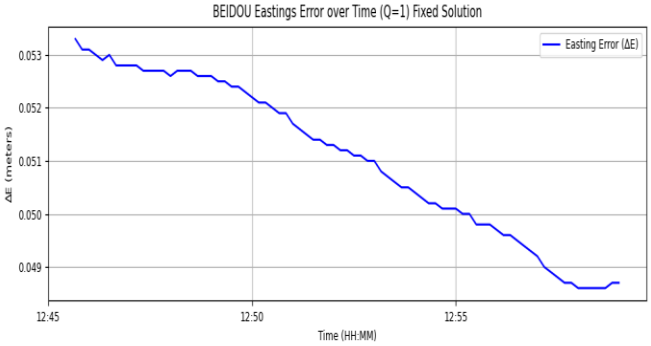

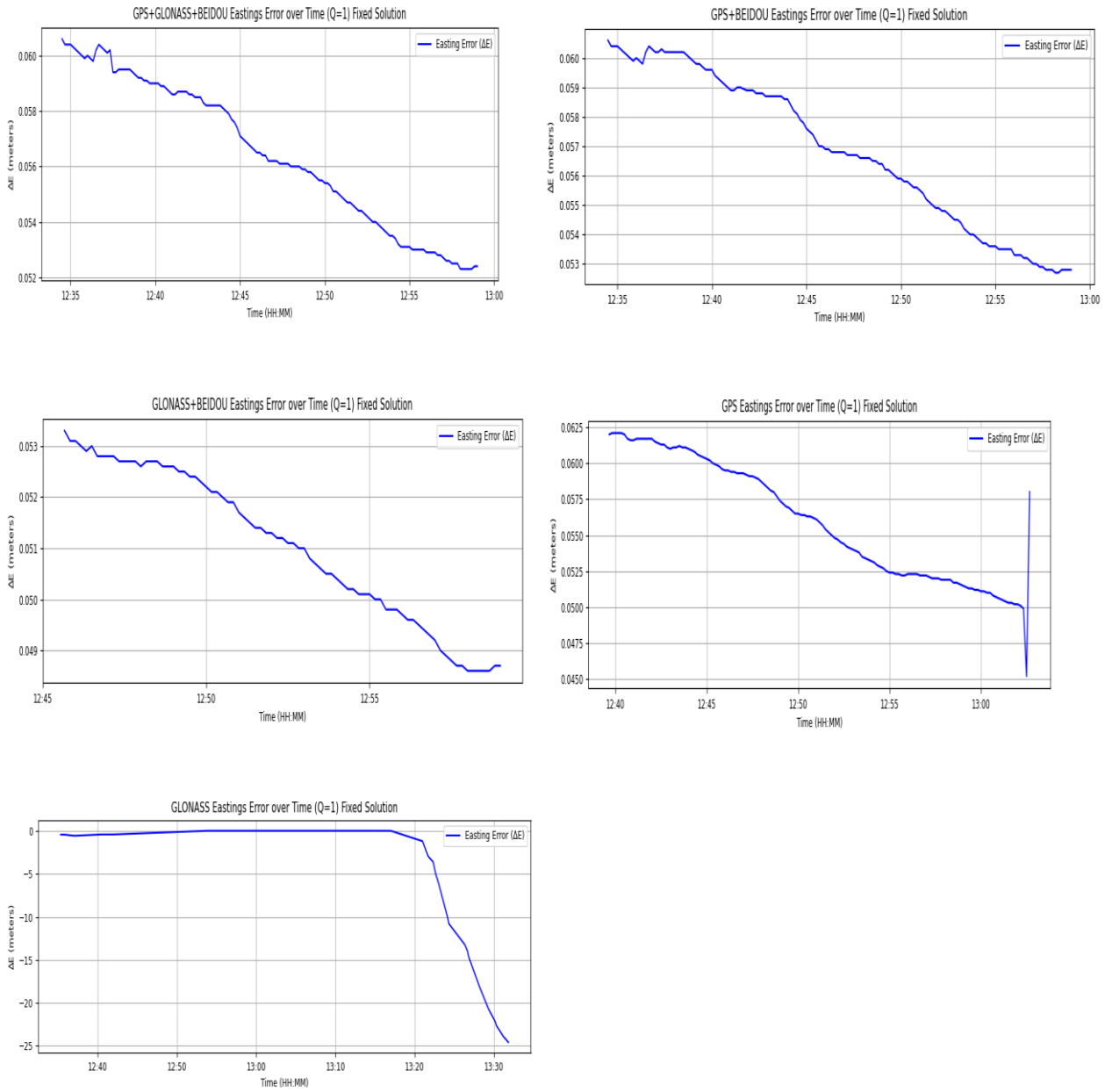

Figure 4.4: Eastings Errors Over Time

4.4.2 Northing Errors Over Time

The time-series graphs for Northing errors show similar patterns to the Easting errors. Most multi-constellation and standalone BEIDOU solutions are very stable, with errors hovering in a narrow band between -0.18 and -0.2 meters, though some show a slight downward then upward curve.

The standalone GLONASS solution is again an outlier, displaying extreme instability with its error skyrocketing from near zero to over 7 meters. The standalone GPS and GPS+GLONASS solutions, while initially stable, also show a delayed degradation, with the errors either spiking or steadily worsening over the observation period.

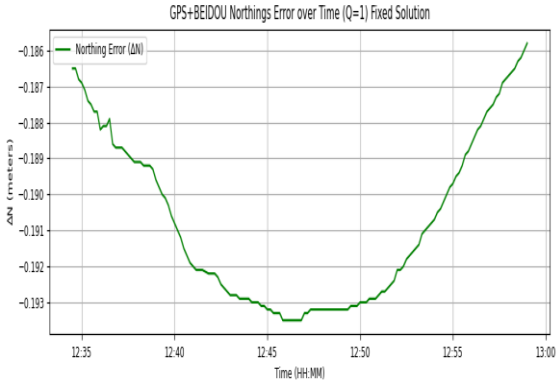

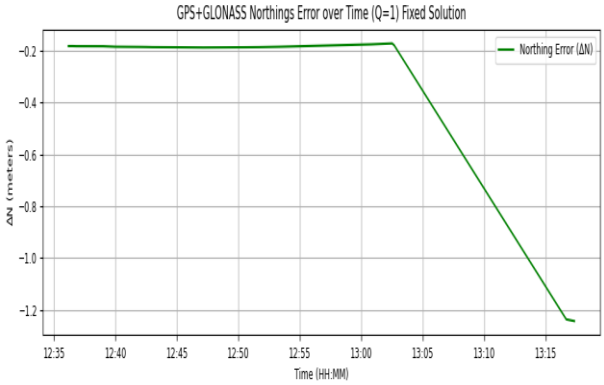

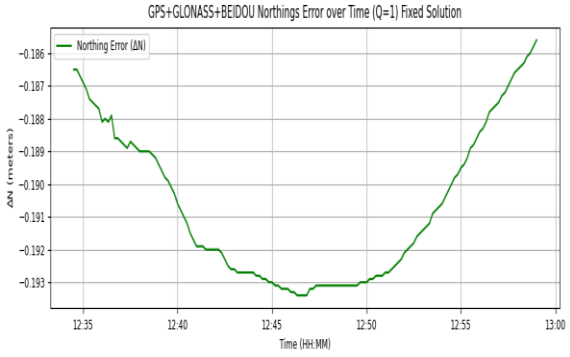

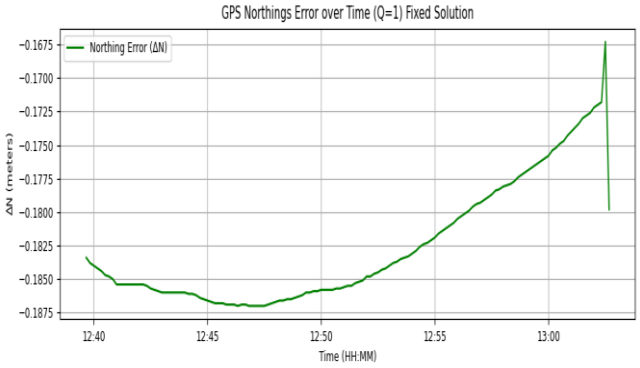

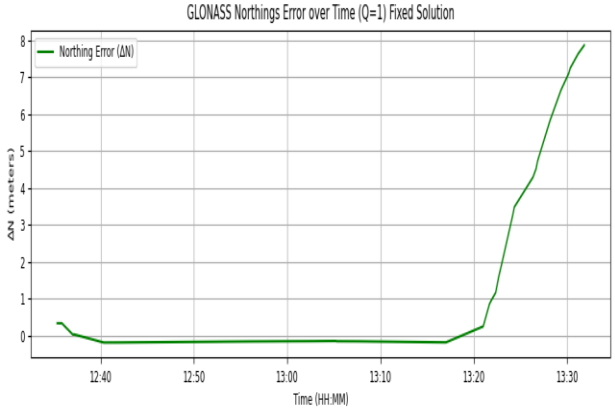

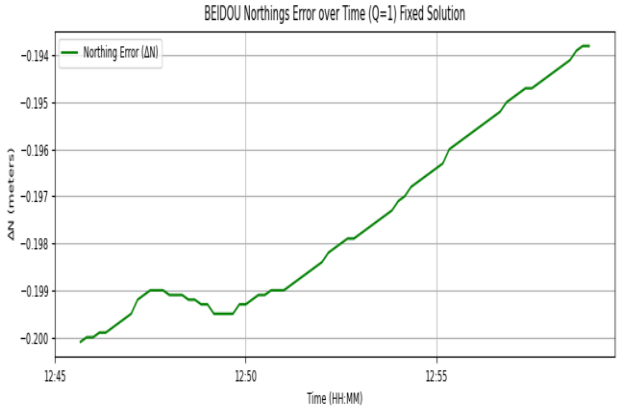

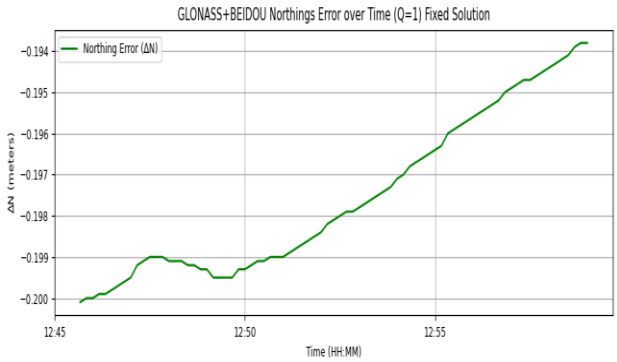

Figure 4.5: Northing Errors Over Time

4.4.3 Number of Satellites Over Time

The stable solutions, like GPS+GLONASS+BEIDOU, which used a high number of satellites (around 17 to 18), and the standalone BEIDOU solution, which consistently used 6 satellites, maintained stable positional errors. Their graphs show a consistent satellite count throughout the observation period. In contrast, the unreliable standalone GLONASS solution, which only used between 4 to 5 satellites, showed extreme instability and a huge error spike that coincided with a sudden change in the satellite count. The sudden error jumps observed in the standalone GPS solution and the GPS+GLONASS combination also directly correspond to abrupt drops and recoveries in the number of satellites used.

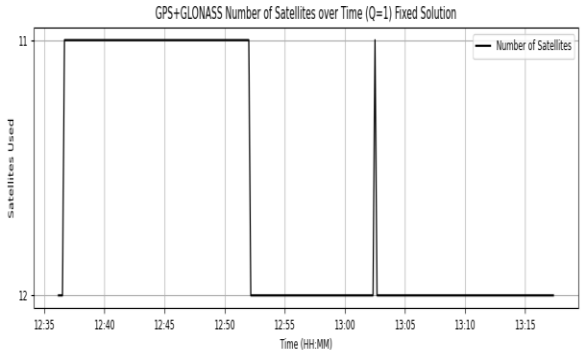

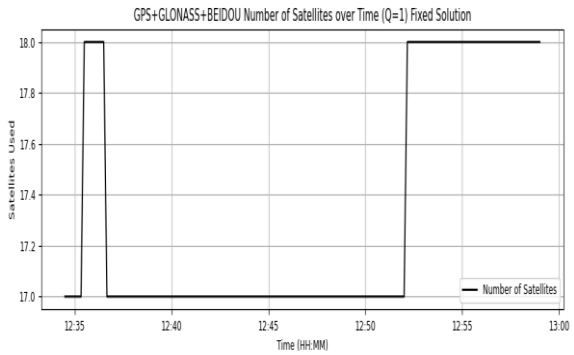

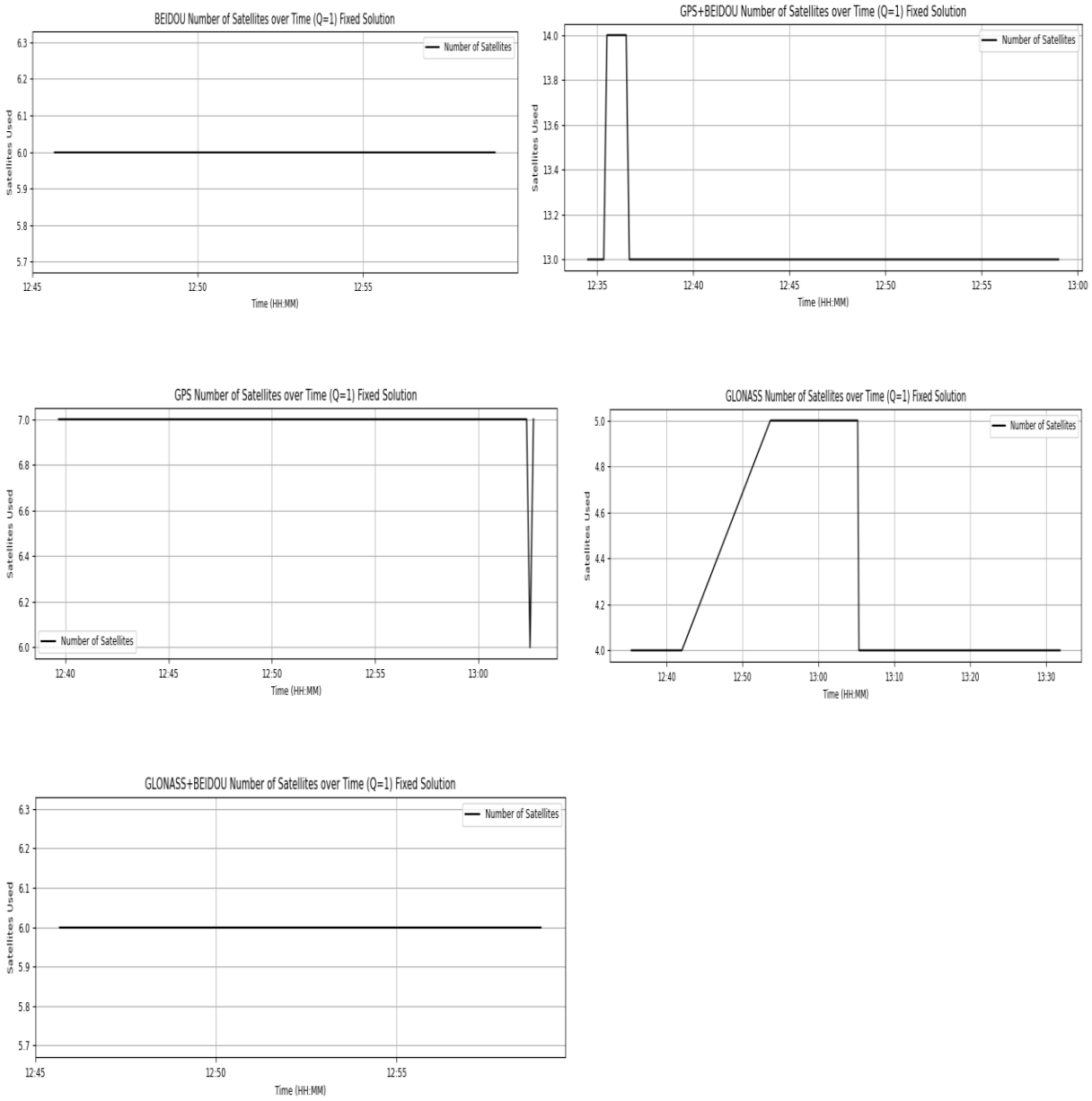

Figure 4.6: Number of Satellites over time

CHAPTER FIVE

CONCLUSION AND RECOMMENDATION

5.1 Conclusion

The primary aim of this research was to investigate the accuracy of post-processed static GNSS data at known control points using a constellation discriminant approach. Based on the comprehensive analysis of data processed through both Tersus Geomatics Office and RTKLIB, this study concludes that the choice of satellite constellation has a profound impact on positional accuracy and stability. The foundational role of the GPS constellation for reliable, high-precision static surveying in the semi-urban environment of Ugbowo Campus is unequivocally confirmed, with GPS-only solutions demonstrating robust performance. While the integration of multiple constellations generally enhances stability, the GPS+BEIDOU combination was identified as the most accurate, achieving the best horizontal metrics. In stark contrast, the significant limitations of standalone non-GPS constellations were exposed, with BEIDOU-only yielding the poorest accuracy and GLONASS-only exhibiting severe instability and extreme errors over time. The time-series analysis further revealed that stable satellite visibility is critical for maintaining positional integrity, as error spikes were directly correlated with drops in satellite counts. Furthermore, the application of robust statistical measures was proven essential for a truthful interpretation of accuracy, given the non-normal distribution of errors across all constellation configurations. Ultimately, for optimal results in similar environments, GPS should form the indispensable core of any surveying strategy, with other constellations like BeiDou serving as valuable augmentations to improve redundancy and geometric strength, rather than as standalone solutions.

5.2 Recommendations

Based on the findings and conclusions of this study, specific recommendations are offered for both Geomatics practitioners and future research directions. For surveyors and GNSS practitioners working in similar semi-urban environments, it is strongly advised to configure receivers with GPS as the foundational constellation, as the GPS+BEIDOU combination proved particularly effective for horizontal accuracy. The standalone use of GLONASS should be avoided for high-precision applications due to its demonstrated instability. Furthermore, integrating robust statistical measures like the Median and Median Absolute Deviation into quality control protocols is recommended to ensure a reliable assessment of accuracy, given the non-normal distribution of errors commonly encountered.

To build upon this work, future research should expand its scope by incorporating the Galileo constellation to provide a fully comprehensive multi-GNSS evaluation. Investigations should also explore the effects of longer observation sessions and different environmental contexts, such as dense urban or open-sky conditions, to develop more generalized best practices. Additional avenues for inquiry include examining the impact of varying baseline lengths on constellation-specific accuracy and leveraging multi-frequency receivers to mitigate ionospheric delays. Finally, a larger-scale study involving a more extensive network of control points would allow for a more rigorous analysis and could identify subtle systematic biases not apparent in this study.

REFERENCES

Abd Rabbou, M., & El Rabbany, A. (2016). Performance analysis of precise point positioning using multi constellation GNSS: GPS, GLONASS, Galileo and BeiDou. *Survey Review, 49*(352), 1–12. https://doi.org/10.1080/00396265.2015.1108068

Abdallah, A., & Schwieger, V. (2015, December 15). PPP for hydrography. *GPS World.*

Akhigbe, R. A., Oladosu, O., & Ehigiator-Irughe, R. (2023). Geodetic control extension at erosion prone areas using integrated CORS–GNSS in Benin City, Edo State, Nigeria. *Dutse Journal of Pure and Applied Sciences, 9*(3b), 255–265.

An, X., Meng, X., & Jiang, W. (2020). Multi-constellation GNSS precise point positioning with multi-frequency raw observations and dual-frequency observations of ionospheric-free linear combination. *Satellite Navigation, 1*(1), 7. https://doi.org/10.1186/s43020-020-0009-x

Angrisano, A., Dardanelli, G., Innac, A., Pisciotta, A., Pipitone, C., & Gaglione, S. (2020). Performance assessment of PPP surveys with open source software using the GNSS GPS–GLONASS–Galileo constellations. *Applied Sciences, 10*(16), 5420. https://doi.org/10.3390/app10165420

Atoki, L. O., Ono, M. N., & Edoki, E. I. (2024). Evaluation of the tropospheric influence on positioning accuracy using IGS RTS data stream compared to static PPP in Abuja, Nigeria. *International Journal of Advances in Engineering and Management, 6*(08), 499–508.

Ayodele, E. G., Okolie, C. J., Ezeigbo, C. U., & Fajemirokun, F. A. (2020). Evaluating the stability and adequacy of NIGNET for the Nigerian geodetic reference frame. *Nigerian Journal of Technological Development, 17*(1), 2–12. https://doi.org/10.4314/njtd.v17i1.1

Ayodele, E. G., Okolie, C. J., Ezeigbo, C. U., & Fajemirokun, F. A. (2020). Evaluating the stability and adequacy of NIGNET for the Nigerian geodetic reference frame. *Nigerian Journal of Technological Development, 17*(1), 3–9. https://doi.org/10.4314/njtd.v17i1.1

Christian U. Ezeigbo. (2022). *Fundamentals of surveying and geomatics.*

Correa Muñoz, N. A., & Cerón Calderón, L. A. (2018). Precision and accuracy of the static GNSS method for surveying networks used in civil engineering. *Ingeniería e Investigación, 38*(1), 35–41. https://doi.org/10.15446/ing.investig.v38n1.64543

Correa-Muñoz, N. A. (2018). Precision and accuracy of the static GNSS method for surveying networks used in civil engineering. *Ingeniería e Investigación, 38*(1), 52–59. https://doi.org/10.15446/ing.investig.v38n1.66055

Dawidowicz, K., & Bakuła, M. (2023). Impact of BeiDou observations on the accuracy of multi GNSS PPP in a function of observing session duration within Europe. *Remote Sensing, 15*(1), 158. https://doi.org/10.3390/rs15010158

DiRita, M., & Hanson, K. (2022). Data fusion for construction monitoring: How Leica Infinity manages images, GNSS data, terrestrial scans and BIM data to efficiently track complex construction sites. *International Archives of the Photogrammetry, Remote Sensing and Spatial Information Sciences, 43*(B2), 373–378.

El-Mowafy, A., Deo, M., & Kubo, N. (2016). Maintaining real-time precise point positioning during outages using a low-cost inertial measurement unit. *Journal of Surveying Engineering, 142*(3), 04015012. https://doi.org/10.1061/(ASCE)SU.1943-5428.0000154

European Commission. (2024, September 18). Successful launch of two new Galileo satellites. Directorate-General for Defence Industry and Space. https://defence-industry-space.ec.europa.eu/successful-launch-two-new-galileo-satellites-2024-09-18_en

European GNSS Service Centre. (2023). *Galileo high accuracy service (HAS).* https://www.gsc-europa.eu/galileo/services/galileo-high-accuracy-service-has

European GNSS Service Centre. (n.d.). *Galileo general introduction.* European Space Agency. https://gssc.esa.int/navipedia/index.php/Galileo_General_Introduction

European Space Agency. (2015). *EGNOS: The European Geostationary Navigation Overlay Service.* https://www.esa.int/Applications/Navigation/EGNOS_the_European_Geostationary_Navigation_Overlay_Service

European Space Agency. (2015). *Steps so far.* https://www.esa.int/Applications/Satellite_navigation/Galileo/Steps_so_far

European Space Agency. (2024, September 17). Two new satellites added to Galileo constellation for increased robustness. https://www.esa.int/Applications/Satellite_navigation/Galileo/Two_new_satellites_added_to_Galileo_constellation_for_increased_robustness

European Union Agency for the Space Programme. (2024, September 2). Galileo is getting ready for the upcoming OSNMA operational declaration. https://www.euspa.europa.eu/newsroom-events/news/galileo-getting-ready-upcoming-osnma

Gao, M., Cao, Z., Meng, Z., Tan, C., Zhu, H., & Huang, L. (2023). Algorithms research and precision comparison of different frequency combinations of BDS 3/GPS/Galileo for precise point positioning in Asia-Pacific region. *Sensors, 23*(13), 5935. https://doi.org/10.3390/s23135935

Gao, W., Zhou, W., Tang, C., Li, X., Yuan, Y., & Hu, X. (2024). High-precision services of BeiDou navigation satellite system (BDS): Current state, achievements, and future directions. *Satellite Navigation, 5*, Article 20. https://doi.org/10.1186/s43020-024-00143-8

Garcia, H. H., Mercurio, M. E., Noveloso, D. P., & Reyes, R. B. (2019). Positional accuracy assessment using single and multi GNSS. *International Archives of Photogrammetry, Remote Sensing and Spatial Information Sciences, XLII-4/W19*, 223–228. https://doi.org/10.5194/isprs-archives-XLII-4-W19-223-2019

Garcia, H. H., Mercurio, M. J., Noveloso, D. P., & Reyes, R. B. (2019). Performance analysis of GNSS positioning using multi-constellation satellites. *International Archives of the Photogrammetry, Remote Sensing and Spatial Information Sciences, XLII-4/W19*, 223–227. https://doi.org/10.5194/isprs-archives-XLII-4-W19-223-2019

GPS World. (2015, January 1). Directions 2015: Galileo looks ahead to early services. https://www.gpsworld.com/directions-2015-galileo-looks-ahead-to-early-services/

Guo, J., Li, X., Li, Z., Hu, L., Yang, G., Zhao, C., Fairbairn, D., Watson, D., & Ge, M. (2018). Multi GNSS precise point positioning for precision agriculture. *Precision Agriculture, 19*(4), 895–911.

Hamza, V., Stopar, B., Sterle, O., & Pavlovčič-Prešeren, P. (2025). Recent advances and applications of low-cost GNSS receivers: A review. *GPS Solutions, 29*, Article 56. https://doi.org/10.1007/s10291-025-01815-x

Hamza, V., Stopar, B., Sterle, O., Krešak, B., Polančič, G., & others. (2025). Recent advances and applications of low-cost GNSS receivers: A review. *GPS Solutions, 29*, 56. https://doi.org/10.1007/s10291-025-01500-2

Herbert, T., Ugochukwu, N. I., & Olatunji, R. I. (2020). Assessing the accuracy of online GNSS processing services and commercial software on short baselines. *South African Journal of Geomatics, 9*(2), 321–330. https://doi.org/10.4314/sajg.v9i2.11

Hou, Z., & Zhou, F. (2023). Assessing the performance of precise point positioning with fully serviceable multi GNSS constellations: GPS, BDS-3, and Galileo. *Remote Sensing, 15*(3), 807. https://doi.org/10.3390/rs15030807

Indian Space Research Organisation. (2023). *NavIC - Indian Regional Navigation Satellite System.* https://www.isro.gov.in/NavIC.html

Jin, S., Wang, Q., & Dardanelli, G. (2022). A review on multi-GNSS for Earth observation and emerging applications. *Remote Sensing, 14*(16), 3930. https://doi.org/10.3390/rs14163930

Kabir, M. S. N., Song, M.-Z., Sung, N.-S., Chung, S.-O., Kim, Y.-J., Noguchi, N., & Hong, S.-J. (2016). Performance comparison of single and multi-GNSS receivers under agricultural fields in Korea. *Engineering in Agriculture, Environment and Food, 9*(1), 53–62. https://doi.org/10.1016/j.eaef.2015.09.002

Karutin, S. (2023, January 6). Directions 2023: GLONASS renews its constellation. *GPS World.* https://www.gpsworld.com/directions-2023-glonass-renews-its-constellation

Leick, A., Rapoport, L., & Tatarnikov, D. (2015). *GPS satellite surveying* (4th ed.). John Wiley & Sons.

Li, X., Li, X., Liu, G., Feng, G., Yuan, Y., Zhang, K., & Ren, X. (2019). Triple frequency PPP ambiguity resolution with multi constellation GNSS: BDS and Galileo. *Journal of Geodesy, 93*, 1105–1122. https://doi.org/10.1007/s00190-019-01229-x

Li, X., Zhang, X., Ren, X., Fritsche, M., Wickert, J., & Schuh, H. (2015). Precise positioning with current multi-constellation global navigation satellite systems: GPS, GLONASS, Galileo and BeiDou. *Scientific Reports, 5*, 8328. https://doi.org/10.1038/srep08328

Malik, J. S. (2020). Performance evaluation of precise point positioning using dual frequency multi GNSS observations. *Artificial Satellites, 55*(4), 263–279. https://doi.org/10.2478/arsa-2020-0011

Marut, G., Hadas, T., Kazmierski, K., & Bosy, J. (2024). Affordable real time PPP—Combining low cost GNSS receivers with Galileo HAS corrections in static, pseudo kinematic, and UAV experiments. *Remote Sensing, 16*(21), 4008. https://doi.org/10.3390/rs16214008

NovAtel. (n.d.). *What are global navigation satellite systems?* https://novatel.com/tech-talk/an-introduction-to-gnss/what-are-global-navigation-satellite-systems-gnss

Odolinski, R., Teunissen, P. J. G., & Odijk, D. (2015). Combined BDS, Galileo, QZSS and GPS single-frequency RTK. *GPS Solutions, 19*(1), 151–163.

Ogutçu, S. (2020). Assessing the contribution of Galileo to GPS+GLONASS PPP: Towards full operational capability. *Measurement, 151*, 107143. https://doi.org/10.1016/j.measurement.2019.107143

Okorocha, C. V., & Olajugba, O. (2014). Comparative analysis of short, medium and long baseline processing in the precision of GNSS positioning. In *FIG Congress 2014 Proceedings* (pp. 1–15). International Federation of Surveyors.

Oladosu, S. O., & Ehigiator-Irughe, R. (2022). Assessment of 3D positional accuracy of geodetic observations from single CORS. *Geological Behavior, 6*(2), 101–106.

Oladosu, S. O., Ehigiator-Irughe, R., & Muhammad, M. B. (2022). Establishment and validation of continuously operating reference stations geosystems network on static and real-time kinematic in Benin City, Nigeria. *Journal of Applied Sciences and Environmental Management, 26*(5), 801–808.

Pan, L., Zhang, X., Liu, J., Li, X., & Li, X. (2017). Performance evaluation of single frequency precise point positioning with GPS, GLONASS, BeiDou and Galileo. *Journal of Navigation, 70*(3), 465–482. https://doi.org/10.1017/S0373463316000771

Pırti, A. (2023). Testing the contribution, accuracy and performance of MGEX positioning in the study region. *Geodesy and Cartography, 49*(4), 222–232. https://doi.org/10.3846/gac.2023.17707

Pırti, A. (2025). Evaluation accuracy, repeatability and performance of Galileo and Beidou positioning in Antarctica region. *Survey Review, 57*(401), 1–15. https://doi.org/10.1080/00396265.2025.2484167

Prol, F. S., et al. (2024). Enabling the Galileo high accuracy service with open source software: Integration of HASlib and RTKLIB. *GPS Solutions.* https://doi.org/10.1007/s10291-024-01617-7

Purfürst, T. (2022). Evaluation of static autonomous GNSS positioning accuracy using single-, dual-, and tri-frequency smartphones in forest canopy environments. *Sensors, 22*(3), 1289. https://doi.org/10.3390/s22031289

Rabbou, M. A., & El Rabbany, A. (2015). Performance analysis of GPS/Galileo PPP model for static and kinematic applications. *Geomatica, 69*(1), 75–81.

Radočaj, D., Plaščak, I., & Jurišić, M. (2023). Global navigation satellite systems as state-of-the-art solutions in precision agriculture: A review of studies indexed in the Web of Science. *Agriculture, 13*(7), Article 1417. https://doi.org/10.3390/agriculture13071417

Romero-Andrade, R., Trejo-Soto, M. E., Vega-Ayala, A., Hernández-Andrade, D., Vázquez-Ontiveros, J. R., & Sharma, G. (2021). Positioning evaluation of single and dual-frequency low-cost GNSS receiver signals using PPP and static relative methods in urban areas. *Applied Sciences, 11*(22), 10642. https://doi.org/10.3390/app112210642

RTKLIB. (2020). *RTKLIB: An open source program package for GNSS positioning.* http://www.rtklib.com/

Septentrio. (n.d.). *Why do you need a multi-frequency multi-constellation GPS/GNSS receiver?* Retrieved May 21, 2025, from https://www.septentrio.com/en/learn-more/about-GNSS/why-multi-frequency-and-multi-constellation-matters

Steer, W. (2021). Precision of static GNSS using multi-constellation data as a function of session length. In *Proceedings of the APAS 2021 Webinar Series.* Australasian Surveyors Congress.

Sunusi, I., Ibaba, A. L., & Oshiga, O. (2024). Analysis of multi-constellation using precise point positioning (PPP) with mobile phone as receiver for coordinate accuracy. *Nile Journal of Engineering and Applied Science, 2*(1).*

Tahsin, M., Sultana, S., Reza, T., & Haider, M. H.-E. (2015, April). Analysis of DOP and its preciseness in GNSS position estimation. In *2015 IEEE ICEEICT.* https://doi.org/10.1109/ICEEICT.2015.7307445

Tersus GNSS. (2024). *Tersus Geo Office 2 user manual.* Tersus GNSS Inc. https://www.tersus-gnss.com/

United Nations Office for Outer Space Affairs. (2023). *Report on the United Nations/Finland workshop on GNSS applications (Helsinki, 23–26 October 2023) (A/AC.105/1303).* https://www.unoosa.org

United Nations Office for Outer Space Affairs. (n.d.). *Global navigation satellite systems (GNSS).* Retrieved May 21, 2025, from https://www.unoosa.org/oosa/en/ourwork/psa/gnss/gnss.html

U.S. Coast Guard Navigation Center. (2023). *GPS space segment.* https://www.gps.gov/systems/gps/space/

Uradziński, M., & Bakuła, M. (2020). Assessment of static positioning accuracy using low-cost smartphone GPS devices for geodetic survey points' determination and monitoring. *Applied Sciences, 10*(15), 5308. https://doi.org/10.3390/app10155308

Wang, L., et al. (2020). Improving the precision and accuracy of wildlife monitoring with multi-constellation, multi-frequency GNSS collars. *Journal of Wildlife Management, 84*(5), 985–1000.

Wired. (2022, August 25). When the UK's timing systems fail, this service will save them. https://www.wired.com/story/satellite-time-distribution

Xia, F., Ye, S., Xia, P., Zhao, L., Jiang, N., Chen, D., & Hu, G. (2019). Assessing the latest performance of Galileo-only PPP and the contribution of Galileo to multi-GNSS PPP. *Advances in Space Research, 63*(9), 2784–2796.

Zhang, J., & Li, W. (2024). Analysis of post processed pseudorange based point positioning with different data sources for the current Galileo constellations. *Sensors, 24*(8), 2472. https://doi.org/10.3390/s24082472